DISTRIBUTION OF HIV-1 DNA IN CD4+ T-CELL SUBPOPULATIONS WITH DIFFERENT CHEMOKINE RECEPTORS

KANTIMA SANGSIRIWUT

อภินันทนาการ

จาก

บัณฑิตวิทยาลัย มหาวิทยาลัยมหิดล

A THESIS SUBMITTED IN PARTIAL FULFILLMENT

OF THE REQUIREMENTS FOR

THE DEGREE OF MASTER OF SCIENCE (MICROBIOLOGY)

FACULTY OF GRADUATE STUDIES

MAHIDOL UNIVERSITY

2000

ISBN 974-664-581-1

Thesis

Entited

DISTRIBUTION OF HIV-1 DNA IN CD4+ T-CELL SUBPOPULATIONS

WITH DIFFERENT CHEMOKINE RECEPTORS

Miss Kantima Sangsiriwut
Candidate

Asst. Prof. Prasert Auewarakul,
M.D., Dr. Med.
Major-advisor

Assoc. Prof. Ruengpung Sutthent,
M.D., Ph.D.
Co-advisor

Prof. Kovit Pattanapanyasat,
Ph.D.
Co-advisor

Prof. Liangchai Limlomwongse,
Ph.D.
Dean
Faculty of Graduate Studies
Mahidol University

Assoc. Prof. Uraiwan Kositanont,
Chairman
Master of Science Programme
in Microbiology
Faculty of Medicine, Siriraj
Hospital
Mahidol University

Thesis

Entited

DISTRIBUTION OF HIV-1 DNA IN CD4+ T-CELL SUBPOPULATIONS

WITH DIFFERENT CHEMOKINE RECEPTORS

was submitted to Faculty of Graduate Studies, Mahidol University

for the degree of Master of Science (Microbiology)

On

August 16, 2000

Miss Kantima Sangsiriwut

Candidate

Asst. Prof. Prasert Auewarakul,

M.D., Dr. Med.

Chairman

Assoc. Prof. Ruengpung Sutthent,

M.D. Ph.D.

Member

Prof. Surapol Suwanagool, M.D.

Member

Prof. Chanika Tuchinda, M.D.

Dean

Faculty of Medicine, Siriraj Hospital

Mahidol University

Prof. Kovit Pattanapanyasat, Ph.D.

Member

Prof. Liangchai Limlomwongse, Ph.D.

Dean

Faculty of Graduate Studies

Mahidol University

ACKNOWLEDGEMENTS

I would like to express the deepest appreciation and gratitude to my advisor, Dr. Prasert Auewarakul for his guidance, invaluable advice, supervision and encouragement throughout my study. I am very grateful to all of my co-advisors, Dr. Reungpung Sutthent, Dr. Kovit Pattanapanyasat, and the external committee, Dr Surapol Suwanagool, for their constructive comments, and critical reading of my thesis. I also would like to thank Mr. Somchard maneenoi for his guidance to the statistical analysis.

I wish to thank all staffs and all my graduate student friends in the Division of Virology, Department of Microbiology, Faculty of Medicine Siriraj Hospital, for their co-operation, generous assistance, and friendship. I also would like to thank the staff of the HIV-Clinic, Siriraj Hospital, for the specimen collection, and very special thanks to all of the patients who donated specimen for this study.

Finally, I am particularly grateful to my family for their support and cheerfulness throughout my study.

<div align="right">Kantima Sangsiriwut</div>

The major HIV-1 chemokine receptors, CCR5 and CXCR4, have been shown to be differentially expressed in subpopulation of CD4+ T cells. CCR5 is expressed mainly on CD45RO memory, activated T cells, while CXCR4 is expressed mainly on CD45RA naïve T cells. To investigate whether viruses with different cell tropism infect different CD4+ T cell subsets *in vivo*, the distribution of HIV-1 proviral DNA in CCR5+CD4+ and CCR5-CD4+ T cell subsets from 30 infected individuals at different stage of disease was determined by competitive nested PCR method. The V1V2 and V3 regions were determined by PCR-direct sequencing and viral phenotype were predicted from the deduced amino acid sequence.

The HIV-1 proviral DNA load in unsorted CD4+ T cells had a broad range from 85 to 6,734 copies/10^5 CD4+ T cells with a median of 389 copies/10^5 CD4+ T cells. There was an inversed correlation between proviral DNA load and CD4 counts ($r = -0.85$, $p = 0.01$, Spearman correlation coefficient).

In all patients HIV-1 provirus could be detected within CCR5+CD4+ and CCR5-CD4+ T cells. The HIV-1 proviral DNA load in CCR5+CD4+ T cells had a broad range from 201 to 3,921 copies/10^5 CD4+ T cells and HIV-1 proviral DNA load in CCR5-CD4+ T cells had a broad range from 24 to 5,157 copies/10^5 CD4+ T cells. The CCR5+CD4+ T cells had a median of two-fold more provirus than CCR5-CD4+ T cells. There was correlation between the ratio of HIV-DNA load in CCR5+CD4+ T cell / CCR5-CD4+ T cell and CD4 count ($r = 0.76$, $p < 0.01$, Spearman correlation coefficient). When comparing the ratio of HIV-DNA load in CCR5+CD4+ and CCR5-CD4+ T lymphocyte subsets, we found that this ratio in patients with CD4 count < 200 cell/mm^3 were less than those in patients with CD4 count > 200 cell/mm^3($p=0.02$, Mann-Whitney U test).

All V3 sequences were grouped as HIV-1 subtype E. Ten of 28 infected individuals were predicted as SI and 18 were predicted as NSI viruses. When comparing the ratio of amount of proviral DNA in CCR5+CD4+ and CCR5-CD4+ T lymphocyte subsets, we found that the ratio in individuals with predicted SI virus were less than in individuals with predicted NSI virus ($p = 0.07$, Mann-Whitney U test). We concluded that NSI or CCR5-using viruses preferentially infect CCR5+CD4+ T cells, while SI or CXCR4-using viruses preferentially infect CCR5-CD4+ T cells.

However, among those samples with low HIV-DNA in CCR5+CD4+/ CCR5-CD4+ ratio, about only half of them showed SI predicted phenotype (4 out of 9 samples with ratio <1 and 10 out of 20 with ratio < 5). We found some patients who were infected by predicted NSI virus had low level of proviral DNA load ratio and low CD4 count. Infact, the sample with the lowest ratio (K18) had predicted NSI phenotype. It might indicate that, the disease might progress even when the viruses remain to be NSI. The infection of CCR5 negative cells by R5 viruses might be due to the ability of these viruses to use CCR5 at subdetectable concentration.

4037130 SIMI/M : สาขาวิชา จุลชีววิทยา วทม. (จุลชีววิทยา)

กันทิมา แสงศิริวุฒิ : การศึกษาการกระจายตัวของดีเอ็นเอของเชื้อเอชไอวี ทัยป์ 1 ใน CD4+ T cell กลุ่มต่าง ๆ ที่มี chemokine receptor ต่างชนิดกัน : คณะกรรมการควบคุมวิทยานิพนธ์ : ประเสริฐ เอื้อวรากุล, MD.,Dr. Med., รวงผึ้ง สุทเธนทร์, MD.,Ph.D., โกวิท พัฒนปัญญาสัตย์, Ph.D. 110 หน้า. ISBN 974 – 664 – 581 –1.

ในการผ่านเข้าเซลล์ของ HIV-1 จะต้องใช้ chemokine receptors บางชนิดในการหลอมเชื่อมระหว่าง envelope ของไวรัสและเยื่อหุ้มเซลล์ของเซลล์ที่มี CD4 พบว่า chemokine receptors ตัวที่มีความสำคัญได้แก่ CCR5 และ CXCR4 เนื่องจากพบว่าถูกใช้โดยไวรัสส่วนใหญ่ chemokine receptors ทั้ง 2 ชนิดนี้มีการแสดงออกในเซลล์ CD4+ lymphocyte ต่างกลุ่มกัน โดย CCR5 จะพบมากบนเซลล์ CD45RO ซึ่งส่วนใหญ่เป็น memory และ activated T cells ในขณะที่ CXCR4 จะพบมากบนเซลล์ CD45RA ซึ่งส่วนใหญ่เป็น naive cells ซึ่งลักษณะที่พบนี้จะมีผลต่อการติดเชื้อของเซลล์ในร่างกายหรือไม่ยังไม่ทราบ เพื่อที่จะทำการศึกษาว่าไวรัสที่มี cell tropism ต่างกัน จะมีการติดเชื้อในเซลล์ CD4+ lymphocyte ต่างกลุ่มกันหรือไม่ ในการทดลองนี้จึงได้ทำการศึกษาการกระจายตัวของ HIV-1 ใน CD4+ lymphocyte 2 กลุ่มคือ CCR5+CD4+ T cells และ CCR5- CD4+ T cells จากเซลล์ของผู้ติดเชื้อ HIV-1 จำนวน 30 คน โดยจะตรวจปริมาณยีโนมของ HIV-1 ใน CD4+ T cells กลุ่มต่าง ๆ ด้วยวิธี competitive nested PCR และได้ทำนาย phenotype ของ HIV-1 โดยพิจารณาจากการเรียงตัวของกรดอมิโนของยีน *env* V1-V3

จากการหาปริมาณของ HIV-1 DNA ใน CD4+ T lymphocyte พบว่ามี DNA อยู่ระหว่าง 85 ถึง 6,734 copies/10^5CD4+ T cells โดยมีค่า median เท่ากับ 389 copies/10^5CD4+ T cell นอกจากนี้ยังพบว่าปริมาณของ HIV-1 DNA นั้นมีความสัมพันธ์แบบผกผันกับค่า CD4 count อีกด้วย (r = -0.85 , p = 0.01 , Spearman correlation coefficient)

ได้ทำการหาปริมาณ HIV-1 DNA ในเซลล์ CCR5+CD4+ และ CCR5- CD4+ พบว่าใน CCR5+ CD4+ T cell มีปริมาณ HIV-1 DNA อยู่ระหว่าง 201 ถึง 3,921 copies/10^5CD4+ T cell และปริมาณ HIV-1 DNA ใน CCR5- CD4+ T cell อยู่ระหว่าง 24 ถึง 5,157 copies/10^5CD4+ T cells และเมื่อทำการเปรียบเทียบค่า HIV-1 DNA ใน CCR5+CD4+ T cell และ CCR5- CD4+ T cell พบว่าใน CCR5+ CD4+ T cell มีปริมาณ HIV-1 DNA มากกว่า CCR-CD4+ T cells โดยเฉลี่ยถึง 2 เท่า พบว่าอัตราส่วนของปริมาณ HIV-1 DNA ใน CCR5+CD4+ T cell ต่อ CCR5- CD4+ T cell มีความสัมพันธ์กับค่า CD4 count (r = 0.76 , p < 0.01, Spearman correlation coefficient) นอกจากนี้ยังพบว่าในผู้ที่เชื้อ HIV-1 ที่มี CD4 count น้อยกว่า 200 cell/mm^3 จะมีอัตราส่วนของปริมาณ DNAใน CCR5+CD4+ และCCR5-CD4+ T cell น้อยกว่าในผู้ติดเชื้อที่มี CD4 count มากกว่า 200 cell/mm^3 (p=0.02, Mann-Whitney U test)

จากการศึกษา sequence ในส่วน V3 ของเชื้อ HIV-1 จากเซลล์ของผู้ติดเชื้อ 28 ราย พบว่าเชื้อทั้งหมดเป็นสับทัยป์ อี จากการทำนาย phenotype พบว่า 10 รายเป็น SI และ 18 รายเป็น NSI เมื่อเปรียบเทียบอัตราส่วนของปริมาณ HIV-1 DNA ใน CCR5+CD4+ T cell และ CCR5-CD4+ T cell พบว่าในผู้ติดเชื้อที่เป็น SI จะมีอัตราส่วนของปริมาณ DNAใน CCR5+CD4+ และCCR5-CD4+ T cell น้อยกว่าในผู้ติดเชื้อที่เป็น NSI virus (p = 0.07 , Mann-Whitney U test) จากการทดลองสรุปได้ว่า NSI หรือ CCR5-using HIV-1 ส่วนใหญ่จะติดเชื้อใน CCR5+CD4+ T cell และ SI หรือ CXCR4 using virus ส่วนใหญ่จะติดเชื้อใน CCR5-CD4+ T cell

นอกจากนี้ยังพบว่าผู้ติดเชื้อบางรายที่เป็น NSI phenotype มีอัตราส่วนของปริมาณ HIV-1 DNA ใน CCR5+CD4+ T cell และ CCR5-CD4+ T cell ต่ำ ซึ่งอาจจะอธิบายได้ว่าผู้ติดเชื้อเหล่านี้อาจจะมีการลุกลามของโรคได้ทั้งๆที่ไวรัสเป็น NSI phenotype ซึ่งอาจเป็นเพราะ R5 virus ในผู้ป่วยดังกล่าวมีความสามารถติดเชื้อในเซลล์ที่มี CCR5 receptor ในระดับต่ำๆ ที่ไม่สามารถตรวจพบได้

CONTENTS

LIST OF TABLES

LIST OF FIGURES

LIST OF FIGURES(Cont)

LIST OF ABBREVIATIONS

Abbreviation or symbol

AIDS	acquired immunodeficiency syndrome
bp	base pair
DNA	deoxyribonucleic acid
dNTP	deoxynucleotide triphosphase
EDTA	ethylene diamine tetraacetic acid
g	gravity
FBS	fetal bovine serum
HIV-1	human immunodeficiency virus type 1
HIV-2	human immunodeficiency virus type 2
Kb	kilobase
mAb	monoclonal antibody
mg	milligram
min	minute
ml	milliliter
ul	microliter

CHAPTER I

INTRODUCTION

The chemokine receptors CCR5 and CXCR4, members of seven-transmembrane G–protein, have been identified as major coreceptors for HIV-1 entry into CD4+ T–cells(1-6).   The coreceptor usage is correlated with viral phenotype and cellular tropisms as well as disease progression.   CCR5 is used as the coreceptor for nonsyncytium inducing (NSI), macrophage-tropic (M-tropic) viruses (2-6), while the other, CXCR4, is used as the coreceptor for T-cell line tropic (T-tropic), syncytium inducing (SI) HIV-1 strains (1,7,8).   The M-tropic and T-tropic viruses are now classified as R5 and X4, respectively (9).   In the early stage of HIV-1 infection most viruses can use only CCR5, whereas during disease progression CXCR4 is also used (10,11).   In vitro data showed that, CCR5 expression was upregulated when CD4+ T–cells were activated with IL-2, while CXCR4 expression was increase during both IL-2 and PHA activation (12).

The expression pattern of both chemokine receptors are different in subpopulations of CD4+ T - cells.   The CCR5 is expressed predominantly on CD45RA-CD45RO+ memory and activated T-cell, whereas CXCR4 is expressed on CD45RA+CD45RO- naïve cells (12-14).   The expression of both chemokine receptors on T-cell subsets suggests that T-cells will differ in susceptibility to different virus strains.   In vitro, memory T-cells are more susceptible to HIV-1 replication than naive T-cells.   However, HIV-1 isolates from patients in late stage of disease progression use CXCR4, which is expressed on naïve cells.   It has been hypothesized that HIV-1

may become more virulent in late stage of infection by gaining wider host range from memory cells to naïve cells. This hypothesis is based on the expression pattern of CCR5 and CXCR4 in CD4+ T-cell subpopulations. Recent studies showed that activated CXCR4+CD4+ T cells increase, especially in later stage of disease progression (15,16). The increasing of CXCR4+CD4+ T cells may render the viral target cell change from CCR5+ T cells to CCR5-CXCR4+ T cells. However, the distribution of virus in these T cell subsets in *vivo* is not known. Consequently, we propose to study the distribution of HIV-1 proviral DNA in different CD4+ T lymphocyte subsets from infected individuals with varied stages of disease. Each T-cell subsets were separated by immunomagnetic separation technique and HIV-1 DNA in these cells were estimated by competitive PCR method. We also studied the correlation between predicted viral phenotype and HIV-1 proviral load in CCR5+CD4+ and CCR5-CD4+ T-cell subset. The V1, V2, and V3 loop sequence were determined by PCR-direct sequencing.

CHAPTER II

Objectives

1. To study the distribution of HIV-1 proviral DNA in CCR5+CD4+ and CCR5-CD4+ T-cell subsets of HIV-1 infected patients using competitive nested PCR.

2. To compare HIV-1 proviral load in CCR5+CD4+ and CCR5-CD4+ T-cell subset from HIV-1 infected individuals with varied CD4 count.

3. To study the correlation between predicted viral phenotype and the distribution of HIV-1 proviral load in CCR5+CD4+ and CCR5-CD4+ T-cell subsets.

CHAPTER III

LITERATURE REVIEW

The human immunodeficiency virus type 1 (HIV-1) was first identified in 1983 and found to be the causative agent of acquired immunodeficiency syndrome (AIDS) in 1984 (17,19,20). In 1983, Barre-Sinoussi and coworkers isolated a virus from lymph node of a patient with persistent lymphadenopathy syndrome (LAS), their virus was called lymphadenopathy-associated virus (LAV) (17,18). In early 1984, Gallo and coworkers reported another human retrovirus, which was isolated from AIDS patients. It was called human T-cell lymphotrophic viruses type III (HTLV-III) (19). At that time, Levy and coworkers also reported another retroviruses. It was recovered from AIDS patients. They called it AIDS-associated retroviruses (ARV) (20). Thereafter, these three viruses (LAV, HTLV-III and ARV) were recognized to be the same virus, which was a member of the *Retroviridae* family and in 1986, the International Committee on Taxonomy of Viruses gave these viruses the name, human immunodeficiency virus, or HIV (21). HIV is subdivided into two types, HIV-1 and HIV-2. HIV-1 is the predominant worldwide isolate from individuals with AIDS or at high risks for the development of AIDS. HIV-2 is endemic among people in West Africa. HIV-1 is divided into three genetic groups called major (M), outlier (O), and nonM-nonO (N). The M group is further subdivided at least eleven subtypes (A to K) on the basis of sequence diversity of full-length genome (22-28).

Transmission of HIV can occur in three ways through contact with infected body fluids such as blood, semen, vaginal secretions, and breast milk. Transmission may

occur across mucous membranes or sexual intercourse (both heterosexual and homosexual), may occur via intravenous exposure such as through sharing infected needles with intravenous drug use, or treatment with infected blood products and from mother to child. Among these, heterosexual contact is the most predominant mode of HIV-1 transmission and responsible for three fourths of all HIV-1 infection worldwide. Now vertical transmission from an infected mother to her child is a special problem. Infection can occur in utero or intrapartum. Postpartum infection can result from the ingestion of breast from an infected mother.

HIV-1 in Thailand was found to belong to 2 subtypes: subtype B and subtype E. Subtype B was first found in 1988 predominantly among intravenous drug users (IDUs) (29). Later in 1989, subtype E spread very rapidly via heterosexual and became predominant subtype in Thailand (30). The increase prevalence among pregnant women is resulting in an increase in vertical transmission and pediatric AIDS.

HIV-1 virion

HIV is a retrovirus of the lentivirus subfamily. The HIV-1 virion is an icosahedral of about 110 nm in diameter. The virion contains a cone-shape capsid, located in the center of the virion, which consists of major capsid protein (CA, p24), nucleocapsid proteins (NC, p6), two identical positive single-strand RNA genome, three viral enzymes, reverse transcriptase (RT), integrase (IN), and protease (PR), and viral accessory proteins Nef, Vif and Vpr. This capsid is surrounded by p17 matrix (MA) proteins, and the entire virion is enclosed in a phospholipid bilayer envelope. The viral envelope (Env) is a lipid bilayer that is derived from the host cellular

membrane. Also incorporated into the envelope is host proteins including HLA Class I and II. The virion gp 120, located on the virus surface, contains the binding sites for the cellular receptors such as CD4 and chemokine receptors and the neutralizing domains. The gp 120 are connected to the virus via interaction with the transmembrane protein (TM, gp 41). Figure 1 shows a diagram of the structure of HIV-1.

HIV-1 genomic organization

The HIV-1 genome size is about 9.8 kb long, with several open reading frames coding for viral structural and accessory proteins. In the proviral state the viral DNA, reverse transcribed from the viral RNA and integrated into the host genome, is flanked on both ends by a long terminal repeat (LTR). The genome contains the three common structural genes: *gag, pol* and *env*. The *gag* (group-specific antigen) gene encodes the structural proteins for the core, while the *env* (envelope) gene encodes the large (160-kDa) precursor viral glycoprotein, gp160, that is cleaved into gp120 and gp41. The *pol* (polymerase) gene encodes several enzymes, including protease, reverse transcriptase and integrase, respectively. HIV-1 also contains two regulatory genes, *tat* and *rev,* which encode Tat and Rev proteins, respectively. The five accessory genes such as *nef, vif, vpr, vpu* and *tev,* which encode Nef, Vif, Vpr, Vpu and Tev proteins, respectively. The genetic map of HIV-1 is shown in Figure2.

Figure 1. HIV-1 virion.

Gene	Main Functions
gag	core proteins
pol	enzymes
env	envelope proteins
tat	positive regulator
rev	differential regulator
vif	infectivity factor
vpr	transcriptional activator
vpu	efficient virus budding
nef	negative regulator
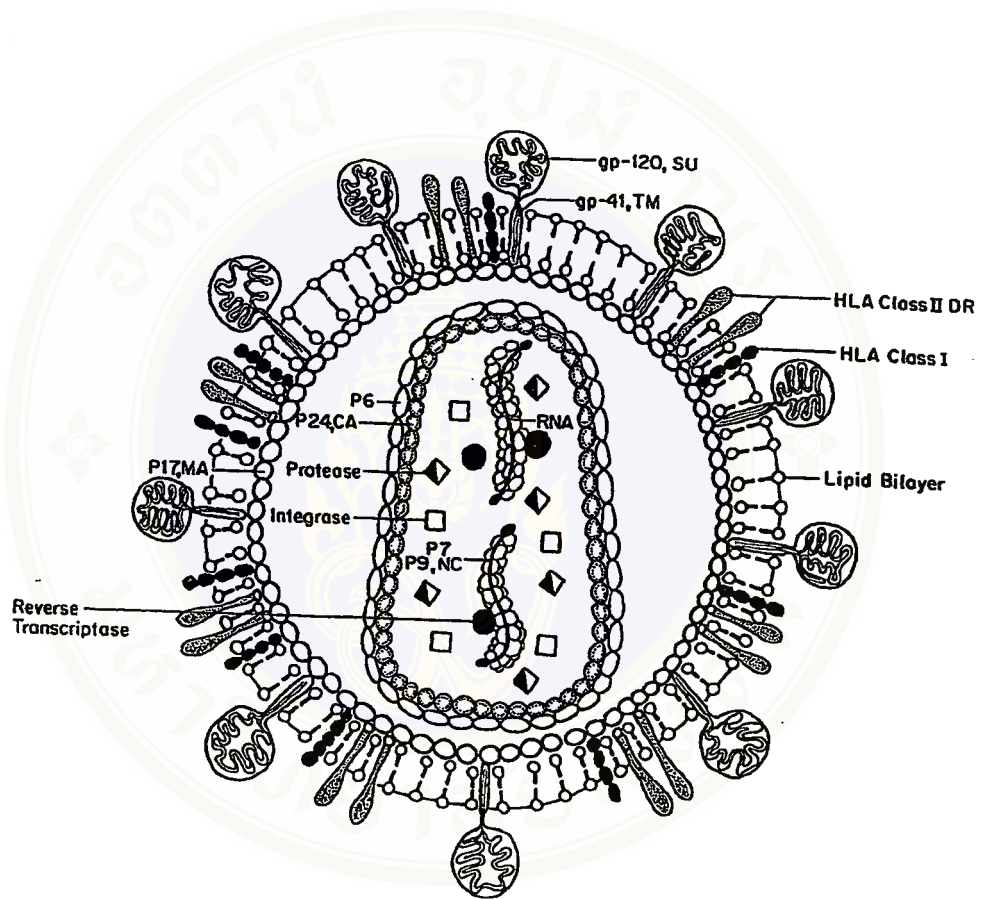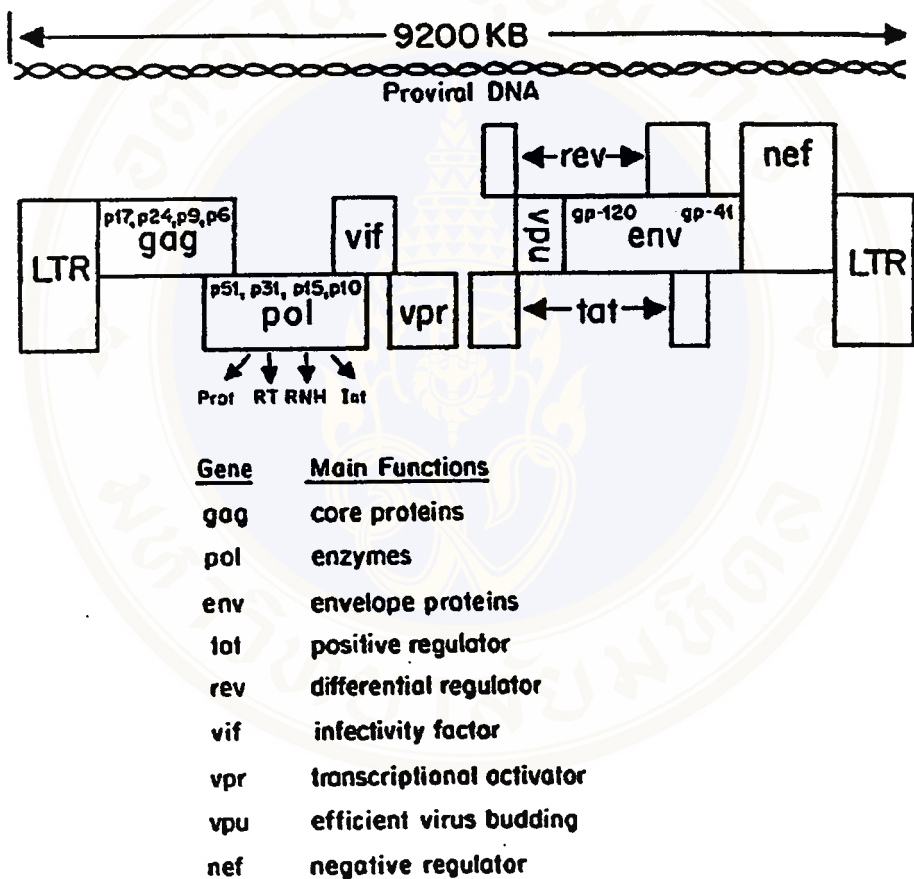
Figure 2. Genetic map of HIV-1. In the proviral stage the viral DNA is flanked on both end by long terminal repeat (LTR). The genome contains three major genes: *gag*, *pol*, *env*, and several accessory genes.

Table 1. Human immunodeficiency virus and simian immunodeficiency virus proteins (From Vincent T. AIDS: etiology, diagnosis, treatment and prevention 4th Ed. Philadelphia NY: Lippincott-Raven Publishers; 1977.)

Name	Size	Function	Localization
Gag MA	p17	Membrane anchoring, Env interaction, nuclear transport of viral core (myristylated protein)	Virion
Gag CA	p24	Core capsid	Virion
Gag NC	p7	Nucleocapsid, binds RNA	Virion
	p6	Binds Vpr	Virion
Protease	p15	Gag-Pol cleavage and maturation	Virion
Reverse Tran-scriptase, Rnase H	p66 p51 (heterodimer)	Reverse transcription, RNase H activity	Virion
Integrase		DNA provirus integration	Virion
Env	gp120/gp41	External viral glycoproteins bind to CD4 receptor	Plasma membrane, virion envelope
Tat	p16/p14	Viral trancriptional transactivator	Primarily in nucleolus/nucleus
Rev	p19	RNA transport, stability and factor (phosphoprotein)	Primarily in nucleolus/nucleus use shuttling between nucleolus and cytoplasm
Vif	p23	Promotes virion maturation and infectivity	Cytoplasm(cytosol, membranes),virion
Vpr	p10-15	Promotes nuclear localization of preintegration complex, inhibis cell division, arrests infacted cell at G_2/M	Virion,nucleus (nuclearmembrane?)
Vpu	p16	Promotes extracellular relase of viral particles, degrades CD4 in the endoplasmic reticulum (phosphoprotein); only in HIV-1 and SIVcpz	Integral membrane protein
Nef	p27/25	CD4 downregulation (myristylated protein)	Plasma membrane, cytoplasm (virion?)
Vpx	p12-16	Virion protein, vpr homologue (not in HIV-1, only in HIV-2 and SIV)	Virion (nucleus?)
Tev	p28	Tripartile Tat-Env-Rev protein (also named Tnv)	Primarily in nucleolus/nucleus

HIV-1 Proteins

Structural Proteins

1.Group specific antigen (Gag)

Gag proteins are derived from Gag precursor (Pr55) and Gag-Pol precursor (Pr160), which are translated from a full-length unspliced mRNA. After viral assembly, Gag precursor is cleaved by the viral protease into four proteins: matrix (p17, MA), capsid (p24, CA), nucleocapsid (p7 and P6, NC). The Pr160 polyprotein is also cleaved into Gag proteins and the viral enzymes: protease, reverse transcriptase and integrase.

MA is the N-terminal component of the Gag polyprotein and is important for targeting Gag and Gag-Pol precursor polyproteins to the plasma membrane prior to viral assembly. MA also helps incorporate Env glycoproteins into viral particles and facilitates infection of non-dividing cell types (31).

CA is the second component of the Gag polyprotein and forms the core of viral particle, with approximately 2,000 molecules of CA protein per virion. HIV-1 capsid is essential role during viral assembly and also functions by binding to the human cellular, an interaction that is essential for HIV-1 infectivity.

NC is the third companent of the Gag polyprotein and coats the genomic RNA as a ribonucleoprotein complex inside the virion core. The primary function of NC is to bind to the packaging signal and deliver full-length viral RNAs into the assembling virion.

2. Pol proteins

The three Pol proteins, PR (protease), RT (reverse transcriptase), and IN (integrase) provide essential enzymatic function and are also encapsulated with in the viral particle.

PR is an aspartic protease and is only active as homodimer. The function of PR is to cleave several polyproteins to produce the MA, CA, NC, and p6 proteins from Gag and PR, RT, and IN proteins from Pol. These processes are essential for viral maturation.

RT is used to generate proviral DNA from viral RNA. RT contains an RNase H domain that cleaves the RNA portion of RNA-DNA hybrids generated during reverse transcription. This enzyme does not has a 3' exonuclease proofreading activity. This results in high mutation rate of one error in 10^4 nucleotides (32).

IN functions to integrate viral DNA into the host chromosomal DNA.

3. Env protein

The HIV-1 Env precursor gp160 is cleaved in the Golgi apparatus by cellular protease into a gp120 external surface envelope protein (SU) and a gp41 transmembrane protein (TM) and two proteins are transported to the plasma membrane for incorporation into virion particle.

The TM consists of an N-terminal ectodomain, a transmembrane domain,and a C-terminal intradomain that interacts with MA. The TM ectodomain structure is a symmetrical trimer, with each monomer consisting of two antiparallel α-helices connected by an extended loop. The overall shape of TM is a rod, with the C and N termini, fusogenic peptide at one end and the extended loop at the other (33). After binding of gp120 to CD4 and chemokine receptor allow to TM releases and reorients parallel to the viral and cellular membranes and permit insertion of the

fusogenic peptide into cellular membrane. This conformational changes in TM leading to membrane fusion (34).

The SU contains five- hypervariable regions (V1-V5) and five conserved regions (C1-C5) are located between the variable regions. The SU core structure consists of two major domains (inner and outer) and a four stranded bridging β-sheet. The inner domain consists of two α-helices, a five-stranded β-sanwich, and several loops. The proximal barrel of the outer domain is a stacked double barrel, with one barrel comprising a six-stranded β-sheet, which twists to enfold helix α2 as a seventh barrel stave. The distal barrel of the stack is a seven-stranded antiparallel β-sheet (34,35). The structure of gp120 as heart-shaped is shown in figure 3. The V3 loop of SU plays an important role in determining of both HIV-1 cellular tropism (36-39) and coreceptor usage (40,41). Numerous studies indicated that CD4 binding induces a conformational change in SU that exposes the chemokine receptor binding surface and enhances interactions with the chemokine receptor and leads to membrane (virus and host) fusion.
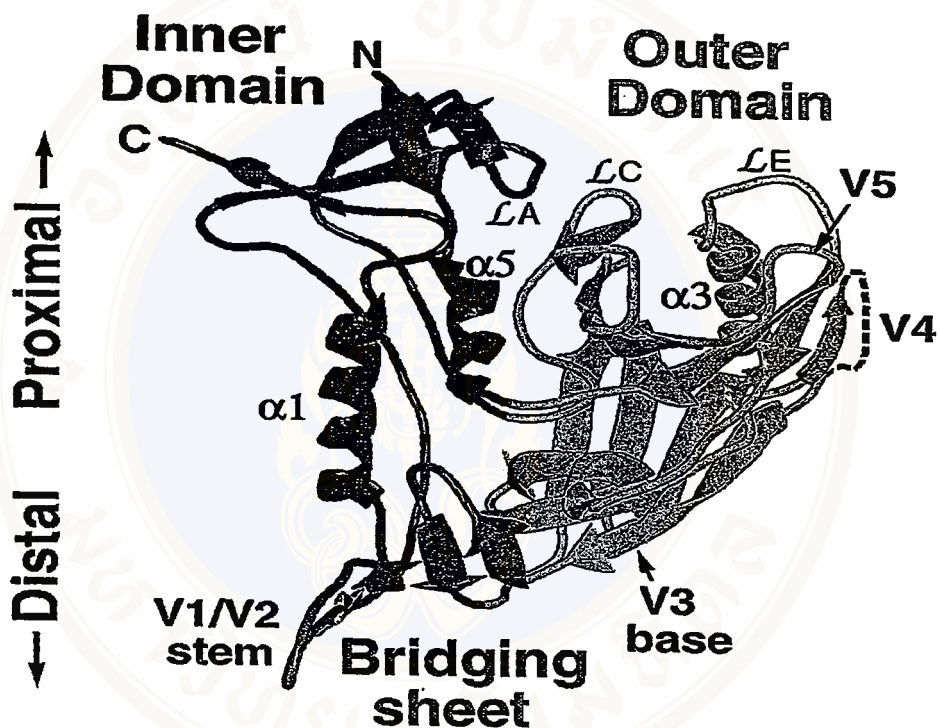
Figure 3. Stereo diagram of an alpha-carbon trace of the gp 120 core (36). The inner and outer domains and the bridging sheet are shown. The inner domain is believed to interact with the gp41 envelope glycoprotein, while the outer domain is believed to be exposed on the assembled envelope glycoprotein trimer. The "proximal" side of the gp120 core, which includes the N- and C-termini, is believed to reside near the viral membrane. The "distal" side of gp120 is believed to face the target cell membrane after CD4 binding occurs.

Regulatory Protein

The Tat protein (transactivator of transcription protein) is a positive regulator of transcription, that increase the level of steady state of HIV-1 RNA transcription by binding to the TAR (trans-activating response element), that located in LTR.

The Rev protein (Regulation of viral protein expression) is required for transportation of unspliced and singly spliced viral mRNAs from nucleus to the cytoplasm by binding at RRE (rev- response element), which is located in *env* gene.

Accessory Protein

The Vif protein (viral infectivity factor protein) enhances efficiency of viral infection, allowing transport of the virus to the cell nucleus and stabilization of DNA intermediates.

The Vpr protein (viral protein R) localizes in nucleus, which is a positive regulator of early viral transcription, promotes transportation of preintegration complex into nucleus, inhibit cell division, and arrests infected cell at G2 phase.

The Vpu protein (viral protein U) is located in membrane, is required for virion release and maturation, and degrades the CD4 molecule in endoplasmic reticulum.

The Nef protein (negative factor protein) has at least two functions: it enhances viral replication and downregulates surface expression of CD4 molecule by endocytosis and lysosomal degradation. The reduction in cell surface CD4 levels important for preventing reinfection by budding virion. In addition, Nef promotes infectivity of cell-free virus.

HIV-1 life cycle

The entry of HIV-1 into cells requires the sequential interaction of the viral envelope glycoprotein, gp120, with a CD4 molecule and a chemokine receptor on the cell surface. HIV-1 entry begins with the viral gp120 envelope glycoprotein binding to the CD4 molecule, which serves as the primary receptor. This interaction results in a conformational change in gp120, which results in exposure of the chemokine receptor binding site. The next step is the interaction of the gp120-CD4 complex with the chemokine receptor, such as CCR5 or CXCR4. Chemokine receptor binding leads to additional conformational change in gp41, that leads to exposure of the hydrophobic amino-terminal region of gp41, which inserts into the cell membrane to initiate membrane fusion (34). Subsequently, the viral nucleoid enters into the cell. Once this stage is achieved, the cycle of viral replicate begins.

The HIV-1 life cycle are shown in Figure 4. After membrane fusion, the virus penetrates the plasma membrane, uncoating, reverse transcriptase converts the genomic RNA into double stranded DNA. The viral DNA is transported to a nucleus and integrated into the cellular DNA as a latent provirus by the viral integrase. When the latently infected cell is activated, the provirus generates spliced and unspliced viral mRNAs transcripts. Viral mRNAs are translated in the cytoplasm, and the Gag and Gag-Pol polyproteins localized to the cell membrane. The Env mRNA is translated at the endoplasmic reticulum. The precursor gag and gag-pol viral polyproteins Vif, Vpr, Nef, and the genomic RNA are assembled into new virus particles at the host-cell surface as immature virion. The viral particle, which buds out of the host cell causing lysis of infected cell. During budding, the viral protease (PR) cleaves gag and gag-pol

precursor proteins to their mature products, generating infectious virions to infect new cells.

The target cells for HIV infection in vitro and in vivo are human CD4 T-lymphocytes and macrophages. The ability of HIV-1 to bind and enter resting and activated CD4+ T cells depends on either the expression of sufficient levels of both CD4 and an appropriate chemokine receptor or viral tropism. Previous studies demonstrated that HIV-1 prefers to infect the memory more than naïve CD4+ T cells (42-44). Although, resting or naive CD4+ T cells allow HIV-1 entry but they are not permissive for the complete viral life cycle and active viral replication. Recent studies have shown that although memory and naïve CD4+ T cells are equally susceptible to infection by HIV-1, but memory CD4+ T cells are able to produce higher infectious virus than naive CD4+ T cells (42,45).
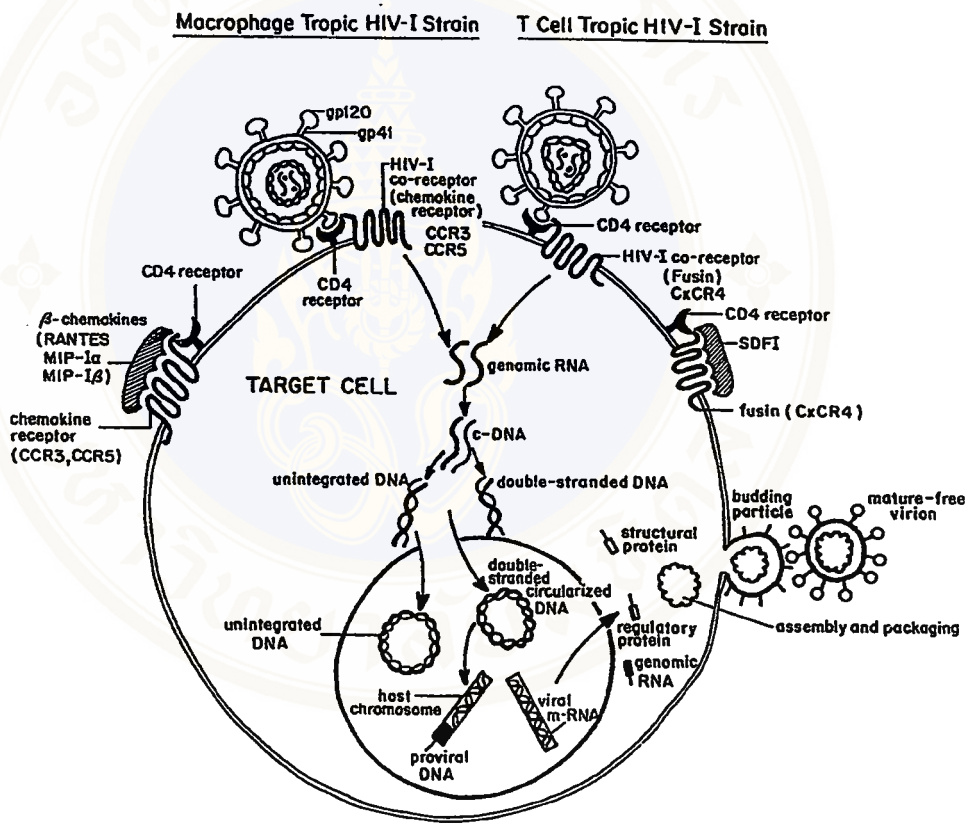
Figure 4. Life cycle of HIV-1. Steps in Viral Replication: Attachment/Entry, Reverse Transcription and DNA Synthesis, Transport to Nucleus, Integration, Viral Transcription, Viral Protein Synthesis, Assembly of Virus, Release of Virus, and Maturation.

Viral dynamic

Understanding viral dynamic requires a steady-state analysis of the amount of free virus and number of infected cells present in infected individuals and dynamic analysis of the rate of virus particles and infected cells are generated and cleared. Recent quantitative viral plasma from HIV-1 infected patients receiving antiretroviral therapy has provided information on the kinetics of virus turnover in vivo. During symptomatic primary infection, levels of infectious virus are very high. The viral load then decreases in association with the development of specific cellular immune responses including the cytolytic T lymphocytes (CTL). During this phase, viral load rangs from 10^2 to 10^7 copies/ml and these levels are constant in individual patients, indicating a steady state or setpoint. Using potent antiretroviral agents to interrupt this steady state between viral and host has provided the understanding of the dynamics of HIV-1 replication. The two main classes of antiretroviral drugs, reverse transcriptase inhibitors and protease inhibitors, both prevent infection of new cells. For reverse transcriptase inhibitors the viral RNA is unable to be reverse transcribed into DNA and the virus is unable to infect the cells. Protease inhibitors prevent infected cells from producing replication-competent virions and new infection of cells is prevented.

Perelson and coworkers monitored the viral load in HIV-1 infected patients after the administration of ritronavir, a potent inhibitor of HIV-1 protease, to describe the dynamic of infected cells and free virus particles (46). After treatment, the viral load in plasma was measured from 2 hours until day 7. They found that the productively infected cells have a mean life-span of 2.21 days ($t_{1/2}$ =1.6 days), and plama virions have a mean life-span of 0.3 days ($t_{1/2}$ =0.24 days). The total virus production is 10.3×10^9 virions/day. The viral life cycle is 1.2 day on average, and that the average

HIV-1 generation time is 2.6 days. This indicates that about 140 viral replication cycles occur each year. The large turnover rate of HIV-1 results in high error rate by reverse transcribtion process. This finding has implication for understanding the evolution of drug resistance mutations and viral escape from immune system.

David Ho and coworkers studied the kinetic of the clearance of free virion from plasma and the loss of virus-producing cells by using combination therapy (47). In this study, infected patients were treated with a protease inhibitor, nelfinavir, and two reverse transcriptase inhibitors, zidovudine and lamivudine. After two weeks of drugs treatment, the plasma HIV-1 RNA level has fallen by around 2 log (99%). There appears to be a change of decline to a slower phase. This slower phase of virus decline is likely to correspond to the dying out of longer-lived virus-producing cells such as macrophages, latent infected lymphocytes, or to the release of trapped virion from the follicular dendritic cells. They studied this phase to estimate the mean half-life ($t_{1/2}$) of long-lived, infected macrophages of 14 days. The mean $t_{1/2}$ of latenly infected CD4 lymphocyte was 1.1 days. They also found 93-99% of the plasma viremia was sustained by productively infected CD4 lymphocyte. These estimated were used to estimate of the amount of time that a patient would need to be treated to eliminate HIV-1 from these compartments. It was suggested that eradication of HIV-1 from infected person might be possible. The potential of prolong combination therapy has the to eradicate the virus depends on the characteristics of these compartments and long-lived reservoirs.

During the asymptomatic phase of HIV-1 infection, plasma viral load reaches a quasi-steady state, with a little change at any time. Thus, at steady state, the rate of production of virus will be proportional to the number of virus-producing cells, and

the virus in blood will be determined by the balance between its rate of production and rate of clearance. It is estimated that HIV-DNA content in peripheral blood lymphocytes ranges from 10^3 - 10^5 copies/10^6 CD4+ T lymphocytes (48,49). Most of these DNA stays as linear unintegrated form in resting CD4+ T lymphocytes. This unintegrated DNA is labile and produced from constant new reverse transcription of new infection in these cells. About 1% of total HIV-DNA in resting cells is found as integrated form. Of these, only minority is replication competent, which is the latent reservoir of the virus. This frequency of CD4+ resting T lymphocytes that carry replication competent HIV-DNA is estimated to be 0.2-16 cells/10^6 lymphocytes. The persistence of replication-competent DNA in a latent form in resting CD4+ T lymphocytes is the major barrier to virus eradication in patients on combination therapy. Majority of HIV-DNA in peripheral blood lymphocytes is defective DNA from accumulated abortive infection in resting cells. Only a small fraction (<0.01%) of the total pool of lymphocytes is productively infected. During the asymptomatic phase of HIV-1 infection, the proportion of cell carrying HIV-1 DNA is three- to tenfold higher in lymph node than in the peripheral blood. The frequency of activated CD4+ T cells carrying integrated HIV-1 DNA in lymph nodes is about 0.02%. And the frequency of resting CD4+ T lymphocytes carrying integrated HIV-1 DNA in lymph nodes is less than 0.05%. Macrophages can be also productively infected by HIV-1 and may function as reservoir for the virus. The mean frequency of lymph node macrophages with integrated HIV-1 DNA was found to be very low (54 per 10^6 macrophages).

Biology of HIV-1

The biologic phenotype of HIV-1 virus is defined by the cell, in which they replicate *in vitro*. Currently three different classification systems are in use. The first defined as macrophage-tropic (M-tropic), T-cell-tropic (T-tropic) and dual-tropic viruses based on their ability infect distinct target cell populations (50,51). The second system definds as either syncytium-inducing (SI) or non-syncytium-inducing (NSI) phenotype (52,53) on the ability of a virus to infect and induce syncytium in the MT-2 cell line (54). The third system definds viruses as either slow/low or rapid/high based on replicative capacity of primary HIV-1 isolates in PBMC (53,55). M-tropic viruses are able to infect both macrophage and primary CD4+ T cells, but unable to infect in T cell line. M-tropic viruses fail to form syncytia in MT-2 cells, replicate slowly in culture and are not associated with rapid progression. T-tropic viruses can infect T-cell-lines, but can not infect macrophage. T-tropic viruses can induce syncytia in MT-2 cells, replicate rapidly in culture and are associated with a rapid disease progression. Dual-tropic viruses replicate in both macrophage and T-cell lines (53,55-58). SI strains are more frequently isolated from patients with full-blown AIDS, whereas NSI strains tend to predominate in recently infected persons.

The discovery of HIV-1 coreceptors allows development of a new classification system based on coreceptor usage. The virus with distinct tropism uses different coreceptor for entry target cells (Table 2). CXCR4 using viruses are SI, T-tropic, whereas CCR5 using viruses are NSI, M-tropic and viruses that use both CXCR4 and CCR5 are dual-tropic viruses (59-62). The CCR5 using, CXCR4 using viruses and viruses that use both coreceptor now called R5, X4, and R5X4 viruses, respectively (9).

Table 2. Coreceptors for HIV-1 infection of CD4$^+$ lymphocytes (From Levy JA.HIV

and the Pathogenesis 2nd Ed. Washington DC: ASM Press; 1998.)

Receptor	Phenotype	Tropism
CCR-5	NSI	Macrophage
CXCR-4	SI	T-cell line
CCR-3[a]	NSI	Macrophage
CCR-2b[a]	SI	Dual-tropic
Bonzo/STRL33[a]	NSI	Macrophage
BOB/GPR15[a]	NSI	Macrophage

[a] Some isolates.

Correlation between biological phenotype and HIV-1 envelope sequences

The third variable region (V3) of the HIV-1 envelope glycoprotein gp120 plays

an important role in determining cellular tropism, cytopathicity and co-receptor usage

(63-66). Previous studies showed that amino acid changes in the V3 region influence

the syncytium-induction of HIV-1. The pattern of amino acid variation in V3 loop can

be used as markers to predict NSI or SI virus for HIV-1. Sequences analysis of the

env gene showed the V3 loop of SI virus contains more positively charged amino acid,

arginine (R) or lysine (K), than that of NSI virus. A positively charged amino acid at

position 306,308 and 320 in gp120 (or 11,13 and 25 in V3 loop) confer SI/CXCR4

using (SI/X4) phenotype, while negatively charged or uncharged confer NSI/CCR5-

using (NSI/R5) phenotype (36,38,63). For HIV-1 subtype E, most of the SI virus

contains predominantly a GPGR or GPGH motif at the tip of the V3 loop instead of

GPGQ. In addition, the loss of a highly conserved N-linked glycosylation site in V3

loop (amino acid at position 6,7,and 8) and the substitution of a bassic amino acid at

position 8 is required for SI viruses (65,67-69).

However, several reports suggest that the V1 and V2 domains may also play a role in determining differences cell tropism and cytopathicity (70-74). The V2 domain appeared to be relatively conserved, particularly in amino acid residues 1 to 29 and 46 to 51. A hypervariable region within V2 was present between amino acid position 29 to 46. The increasing number of N-linked glycosylation site of V2 region were previously reported to be associated with the SI phenotypes (70). Nevertheless, other researchers reported there was no difference in the number of N-linked glycosylation site in V1 and V2 region between SI and NSI phenotypes (75). V2 extensions were also reported to be associated with the SI phenotypes (70). However, other groups have not found the correlation between the length of V2 region and SI or NSI phenotypes (75-76).

Table 3. Characteristics of V3 loops sequences of NSI and SI virus

Virus Phenotype	V3					
	Charge of amino acid position			V3 motif	N-link glycosylation site N-X-S/T	Net charge
	11	13	25			
SI	Positive	Positive	positive	GPGR or GPGH	1	≥5
NSI	Negatie/ unchare	Negatie/ unchare	negativ/ unchare	GPGQ	0	≤4

Chemokine and Chemokine receptors

The primary receptor for human immunodeficiency virus type 1 (HIV-1) is CD4. However, only CD4 molecule is not sufficient for HIV-1 entry into cells. Several studies showed that, CD4-expressing nonhuman cells fail to make them permissive for virus infection (77-79). These studies suggest that the virus requires a second receptor for fusion and entry into its target cell. In 1996, Berger and coworkers found a cDNA cloned from a human continuous cell line (HeLa) that expressed a protein, designated fusin (1). When fusin was introduced into HIV-resistant mouse cells expressing human CD4, they became susceptible to HIV infection. Fusin is now called CXCR4 receptor that acted as a co-receptor for T-cell tropic, SI HIV-1 strains. Therefore, the T-cell tropic virus strains that require CXCR-4 have recently been renamed X4 viruses. In the same year, five independent groups reported that CCR5 was a co-receptor for M-tropic, NSI HIV-1 strains (2-6). CXCR4 and CCR5 are member of the seven-transmembrane G-protein-coupled receptor family. CXCR4 is a receptor for the α-chemokine, while CCR5 is a receptor for the β-chemokine. SDF-1 is the natural ligand for CXCR4 can block the ability of CXCR-4 to serve as a co-receptor for T-tropic strains of HIV (7-8). The β-chemokine, regulated-on activation normal T-cell expressed and secreted (RANTES), macrophage inflammatory protein (MIP)-1α and MIP-1β, are natural ligands for CCR5(2-4). CCR5 receptor binding by these chemokines inhibited M-tropic virus infection of CD4^{+} cells. In addition to CCR5 and CXCR4, at least nine other chemokine receptors have been shown to support the cellular entry of one or more virus strains. These include CCR2b, CCR3, CCR8, GPR1, GPR15, STRL33, US28, V28, and ChemR23 (80-87).

HIV-1 coreceptor use

CCR5 using viruses (R5 viruses) are associated with HIV-1 transmission by sexual contact, the transfer of infected blood or blood products, and predominate in early and all stage of infection. During the course of disease, about 50% of infected individuals, CCR5 using viruses can evolve to use CXCR4 receptor (R5X4 or X4 viruses). The emergence of these viruses is correlated with a decline of CD4+ T cells, an increase in viral load, and disease progression to AIDS (10,11).

Role of coreceptor in HIV-1 transmission and disease progression

The role of coreceptor for HIV-1 transmission is demonstrated by a polymorphism of CCR5, which are called CCR5Δ32. CCR5Δ32 has a 32 bp deletion in the second extracellular loop, causing a stop codon in transmembrane domain 5. The truncated protein product is not expressed on the cell surface (88,89). People who are homozygous for ΔCCR5 are highly resistance to HIV infection with R5 but not X4 or R5X4 viruses (89,90). The individuals who are ΔCCR5 heterozygous (CCR5/Δ CCR5) have delay AIDS onsets when compare to individuals with wild-type alleles (90,91). The CCR5 mutation is genetically inherited and is common in Caucasians but uncommon in the Middle East and India and only sporadically found among native Africans, Americanindians, and East Asians. About 1% Caucasian people are homozygous and 10% are heterozygous (89,90). So far other two coreceptor/chemokine genetic polymorphisms have been identified and correlated with delayed HIV-1 disease progression rate: CCR2-64I and SDF-1 3'A (92,93). The CCR2-64I polymorphism is an amino acid change, valine to isoleucine, at position 64 in the first transmembrane domain of CCR2. This allele is found in Caucasians, frican

Americans, Hispanics, and Asian about 10%, 15%, 17%, and 25%, respectively. The CCR2-64I has no effect on HIV-1 transmission but this allele correlates with delay progression to AIDS (92). The SDF-1 3'A allele is a base change, G to A, at bp 809 of the 3'-UTR of the mRNA for SDF-1β. SDF-1 3'A is found in Caucasians (21%), Hispanics (16%), Asian (26%), and African Americans (6%). The homozygotes 3'A/3'A is associated with delayed disease progression (93).

Expression and regulation of CXCR4 and CCR5

Two major HIV-1 co-receptors, CXCR4 and CCR5 are the predominant used in HIV-1 entry. Their expression pattern is important for determining viral tropism and HIV-1 pathogenesis. The importance of CCR5 for HIV-1 transmission is shown in individuals homozygous for the Δ32-CCR5 allele, who have no surface expression of CCR5 and is highly resistance for HIV-1 infection. In contrast, individuals with Δ32-CCR5 heterozygous have lower CCR5 expression levels and progress to AIDS more slowly than individuals without this allele.

CD4 T-lymphocyte cells can be subdivided into naive and memory subset depended on cell surface marker. Naive T cells have not yet exposed to antigen and express CD45RA while memory T cells have been exposed to antigen and express CD45RO. Chemokine receptor expression on T-lymphocyte subsets has been examined in vitro using monoclonal antibodies. Chemokine receptors CXCR4 and CCR5 are expressed differentially on CD4 T-lymphocyte subsets. Previous studies have demonstrated that CXCR4 was expressed predominantly on CD26 low, CD45RA+, CD45RO- T cells, indicating a naïve inactivated phenotype, whereas

CCR5 was expressed predominantly on CD26 high, CD45RA-, CD45RO+ T cells, indicating a memory cells (12,15).

The chemokine receptor that expresses on the cell surface of monocytes is CXCR4 (94,95), however differentiation of monocyte to macrophage induces CCR5 expression.

The chemokine expressions have been shown to be differentially regulated in vitro depending on the activation stimulus (12). Phytohemagglutinin (PHA) was shown to down-regulate CCR5 and up-regulate CXCR4, whereas interleukin-2 (IL-2) was shown to up-regulate CCR5 and CXCR4 expression. The other researcher reported, the expression level of the coreceptor relative to CD4. When CD4 is expressed on the cell surface at high levels, low levels of CCR5 or CXCR4 are need for virus entry. However, if CD4 is expressed at low levels, high levels of the coreceptors are needed (96).

Surrogate markers for disease progression

A variety of immunologic and virologic markers have been used to study the pathogenesis, to predict the clinical outcomes of HIV-1 infected patients, and to assess the efficacy of antiretroviral therapy (97). Historically, the most commonly used methods include absolute CD4 count, serum HIV-1 p24 antigen, and quantitative microculture of HIV-1 from plasma or PBMCs.

Serum HIV-1 p24 antigen was the first marker used in the study of HIV disease and to assess the effects of antiretroviral treatment. However, p24 antigen can not be detected in patients in early stages of HIV disease. Furthermore, levels of HIV-1 p24 antigen are not correlated with the rate of viral replication (98).

Quantitative microculture techniques were developed to measure HIV-1 in plasma or PBMCs of HIV patients. These assays are useful markers of disease progression, and to assess the effect of antiretroviral therapy. However, these techniques have low sensitivity. They can detect HIV-1 in only about 25% of asymptomatic HIV infected patients (99).

A potentially important prognostic marker is viral phenotype. Previous studies reported SI virus correlate with low CD4 count and HIV-1 related disease. HIV-1 positive individuals with long-term asymptomatic infection usually harbor NSI virus. However, NSI viruses can be detected throughout HIV-1 infection, but SI viruses usually detect only during the course of HIV-1 infection and disease progression to AIDS.

Several studies used proviral DNA for prognosis of HIV infection, the result showed that an increase in proviral DNA correlated with disease progression. In nonprogressors had lower proviral DNA than rapid progressors (99-102). Now PCR is a powerful amplification technique that is capable of identifying very low copy numbers of proviral DNA and it can be detected readily.

Recent studies used quantitative plasma HIV-1 RNA levels to predict clinical progression and to assess the effects of antiretroviral treatment. Patients with a high levels of plasma HIV-1 RNA at baseline progress faster to AIDS or death than patients with lower levels. Plasma HIV-1 RNA levels decrease rapidly in patients beginning anti-retroviral therapies and rise again when therapy is discontinued or drug resistance develops. At present, there are three commercially available for quantitative viral RNA including branched DNA (bDNA) Signal Amplification, RT-PCR, and Nucleic Acid Sequence Based Amplification (NASBA).

Quantification of HIV-1 DNA by competitive polymerase chain reaction

Quantitative competitive polymerase chain reaction (cPCR) has been developed to measure HIV-1 DNA in clinical specimens (101,103). In this assay, a DNA fragments of the same primer recognition sequences as a target DNA of sample, except for a deletion or a insertion, are used as competitors for quantitative PCR. The competitor that serves as an internal standard control for PCR assay and acts as control for amplification efficiency. The target DNA and the competitor are coamplified with in tha same tube and share the same primers. The cPCR is performed by the addition of increasing amounts of known copy numbers of competitor to equal amounts of target DNA, and quantification is determined by the relative amounts of amplification product derived from the target DNA and the competitor DNA. Quantitative PCR with DNA competitor is useful in the detection and quantification of low amounts of DNA (104). In addition, the competitor has been cloned into a plasmid vector downstream to T7 RNA polymerase promoter. The construct can be used to produce RNA competitor for further development of a competitive PCR for HIV-1 RNA viral load measurement.

Cell separation using surface markers

The separation of cells has become more important both in basic research as well as in clinical sciences. Cell separation is the process of separating cells of interest from other cells. The goals of cell separation are purity, recovery and cell viability. Earlier methods are based on cell characteristic such as cell size, density, and affinity. Since monoclonal antibodies (mAbs) against cell surface marker are developed, cell separation techniques based on cell specific surface markers are widely used.

Currently three different methods are in use. The first is an affinity chromatography /panning. These methods use anti-antibody bind to the column or plastic plate for separation the cell with specific mAb. These methods have high recovery but low purity. The second method is immunomagnetic bead separation, in which interested cells are labeled with magnetic bead and labeled cells are separated by attraction to the magnet. These methods are very simple for use but they have lower cells purity than FACS. The third method is fluorescence-activated cell sorting (FACS). In this method the interested cells are labeled with antibody conjugated with fluorescent dyes, and separation base on the charge and deflection of the labeled cell. All of this method FACS provides highest purity and recovery but it requires expensive machine, expertise and their capacity are limited for handling large cell numbers.

CHAPTER IV

MATERIALS AND METHODS

Subjects

The subjects in this study were 30 HIV-1 infected individuals who sought medical care at HIV-clinic of Siriraj Hospital during October 1999 – March 2000. None of all subjects received antiretroviral drug therapy. Ten milliliters of peripheral blood were collected in sterile EDTA vacutainer tubes and processed within 3 hours after collection. All of specimens were also determined for CD4 count.

Sample preparation

Two hundred microliters of whole blood were set aside for immmunofluorescent staining. Then the whole blood sample was centrifuged at 1,500 rmp for 10 min to separate plasma and cell. The plasma was discarded. The blood cells were diluted with equal volume of 1X phosphate buffer saline (PBS). Diluted blood cells were layered over one-third volume of Ficoll-hypaque solution (Isoprep, Robbins Scientific, CA, USA) in a 15 ml centrifuge tube. The tube was then centrifuged at 1,500 rmp for 20 min without break. Peripheral blood mononuclear cells (PBMCs) were harvested from the interface of the gradient and transferred to a new 15 ml centrifuge tube containing 8 ml of 1X PBS. The cell suspension was centrifuged at 1,000 rpm for 10 min to wash the PBMCs. The supernatant was discarded and the cell pellet was washed 2 times with 5 ml of 1X PBS, and resuspended in 5 ml of RPMI 1640 with 10%FBS in a 25 cm^2 tissue culture flask (Nunc,Denmark). The cells were incubated

overnight at 37°C with 5%CO_2 in a 25 cm^2 tissue culture flask to get rid of monocytes. The non-adherent cells were collected and washed in 1XPBS and resuspend in 1 ml of 1X PBS. The cells were counted with hemocytometer (KOVA Glassitc slide 10). Three million PBMCs were collected in 1.5 ml sterile microtube, stored at -20°C until use for PCR. Twenty thousands non-adherent cells were stained with anti CD14-CD45 to determined monocytes contamination. The remained PBMCs were used for purification of T-lymphocyte subsets.

Immunofluorescent staining and flow cytometry analysis

Fifty microliters of whole blood was stained with 7 µl of anti-CD4 (Becton Dickinson, San Jose, CA) for 15 min at room temperature. The red blood cells were then lysed in FACS® lysing solution (BD) for 10 min at room temperature, washed, resuspend in 1XPBS with 1% paraformaldehyde, and kept at 4°C until analyzed with flow cytometry within three days.

Fifty microliters of whole blood was stained with 0.5 µl of 0.5 µg/ml of anti-CCR5 (2D7)(Pharmingen) for 15 min at room temperature. Negative control with out anti-CCR5 was processed in parallel. The cells were washed twice in 1XPBS and centrifuged at 1,200 rpm for 5 min. The supernatant was discarded and the cells were incubated with 3 µl of FITC-conjugated goat anti-mouse immunoglobulin (Becton-Dickinson) for 15 min at room temperature. After incubation the cells were then washed twice in 1XPBS and incubated with 6 µl of PE-conjugated anti CD$_4$ (BD) at room temperature for 15 min. The red blood cells were then lysed in FACS® lysing solution (BD) for 10 min at room temperature, washed, resuspend in 1XPBS with 1%

paraformaldehyde, and kept at 4°C until analyzed with flow cytometry within three days.

Flow cytometry analysis was performed on a FACSort (BD) using CellQuest (BD) software. The stained cell were collected on 10,000 events of each sample and gated by their forward-scatter and side-scatter.

Cell Separation with MACs

Magnetic Labeling

Nonadherence cells were washed with 1XPBS supplemented with 0.5% bovine serum albumin (BSA) and 2 mM EDTA. Three million cells were collected as pre-separated cell. The remained cells were resuspened in 500 µl of PBS and filtered by passing through a filter with pore size 30 um (Miltenyi, Germany) to remove clumped cells. Eight million cells were resuspened in 92 µl of 1XPBS and incubated with 8 µl of 0.5 µg/ml of anti-CCR5 (2D7) for 15 min at 4°C. The stained cells were washed two times with 1XPBS. The cell pellet was resuspened in 84 µl of 1XPBS and incubated with 16 µl of MACS anti-immunoglobulin MicroBeads (Miltenyi, Germany) for 15 min at 4°C in order to label the cells magnetically. The labeled cells were washed with 1XPBS and resuspened in 500 µl of PBS and proceeded to magnetic separation.

Magnetic Separation

A MiniMACS magnet (Miltenyi, Germany) was attached to a MACS MultiStand (Miltenyi, Germany). A separation column (Miltenyi, Germany) was attached to a flow resistor and placed in the magnet. Five hundreds microliter of 1X PBS was added in the column. The effluent was discarded. The magnetically labeled

cells were applied onto the column. The cells that passed through the column were collected as negative cells. The cells that retained in column were washed three times by adding 500 μl of 1XPBS. After washing, the column was removed from the magnet and placed on a collection tube. The positive cells that retained in column were eluted with 1 ml of 1XPBS by flushing with gentle pressure using a plunger. The positive cells were re-separated in a new column in order to maximize purity. The separation was performed under the same condition as the first round.

After cell separation, $1-2 \times 10^4$ cells of each fraction (before separation, negative and positive fraction) were stained with FITC-conjugated with goat anti mouse antibody and analyzed by flow cytometer to assess purity. Twenty thousands cells of CCR5 negative fraction were stained with anti CXCR4, FITC-conjugated with goat anti mouse antibody and analyzed by flow cytometer to assess CXCR4 expression. The remained cells of each fraction wee kept at $-20^{\circ}C$ until used.

Construction of competitor DNA

A competitor was generated by using PCR mutagenesis and overlap extension method. Plasmid pHXB2 was used as template. First, pSKAN was constructed as previously describe (105). Briefly, pHXB2 was amplified with the SK38Δ-SK39 primes. The SK38Δ including 18 bp deletion from position 1579 to 1596, as shown in Figure 5 &Table 4. Subsequently, this product was amplified again with the SK38-SK39 primers in order to add the 5' end of SK 38 primer site. Second, a K1 fragment with internal 18 base deletion was generated using purified pSKAN and SK390 as primers. PCR reaction mixture consisting of pHXB2 as template, purified pSKAN and SK390 as primers, 1Xstandard PCR buffer and 1.5 mM $MgCl_2$ (10 mM Tris-

HCl,50mM KCl and 0.1% Triton®X-100) was denatured at 100 °C for 10 min, then chilled on ice and 200 μM each of dNTPs and 2.5U Taq DNA polymerase were added. This long denaturation was to increase the chance of hybrid annealing (106). Amplification were carried out in 35 repeated cycles consisting of 95 °C for 1 min, 60 °C for 1 min and 72 °C for 1 min and additional cycle at 72 °C for 10 min. Finally, the competitor was made in another PCR reaction with pHXB2 as template, SK380 and purified K1 as primers. Amplification was done under the same conditions as described for K1 synthesis. A large amount of DNA competitor was purified and quantitated by using UV spectrophotometer and visual intensity of ethidium bromide fluorescent of DNA by Saran wrap method (107). The copy number of competitor was then calculated based on molecular weight of the competitor genome and Avogadro number as follow

$$\text{Copy of competitor(copy/}\mu l) = \frac{\text{Avogado number x Concentration of competitor}(\mu g/\mu l)}{\text{Molecular weight of competitor (Kg) x } 10^9}$$

Avogado number $= 6.02 \times 10^{23}$

Molecular weight of competitor = 135 Kg

Table 4. Oligonucleotide primers for competitor construction and nested PCR

Gene	Primer	Sequence (5'→3')	Location
gag	SK38Δ	CCTATCCCAGTAGGAGAAATC CTGGGAT TAAATAAAATAGTAAG	792-836[a]
	SK380	GAGAACCAAGGGGAAGTGACATAGCAGG	684-712[a]
	SK390	TAGAACCGGTATACATAGTCTCTAAAGGG	903-874[a]
	SK38	ATAACCACCTATCCCAGTAGGAGAAAT	784-811[a]
	SK39	TTTGGTCCTTGTCTTATGTCCAGAATGG	870-898[a]
env	ENV B	AGAAAGAGAAGAAGACAGTGGAAATGA	6191-6217[b]
	AO2	GGAATTCAAAGGTGAGTATCCCTG	8335-8358[b]
	AI1	GGGATCCTTATTATGGGGTTCCTGTGTGG	6317-6345[b]
	AI2	GGAATTCTTCCCTCCTCCAGGTCTGAA	7609-7635[b]
	CI1	GGGATCCGGCAGTCTAGCAGAAGAAGAGA	7012-7040[b]
	BI2	GGAATTCTAGATCTCCTCCTGATGGTGGCTGAA	7301-7333[b]
	PV1	CAGATGCAGGAGGATGTAATCAGT	6513-6540[b]

[a] according to HIV clone HXB2

[b] according to HIV-1 clone 93th253, GenBank Accession number U51189
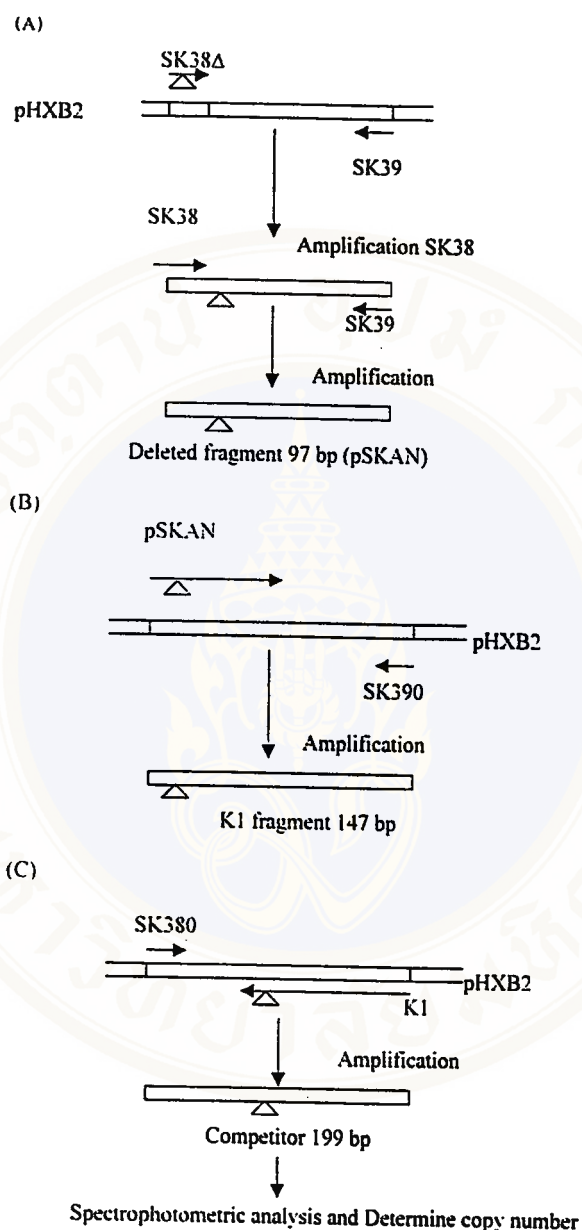
Figure 5. Schematic diagram representation of the construction of a competitor DNA. Plasmid pHXB2 was used as template for PCR to generate the competitor. PCR primers are listed in table 1. For generation of pSKAN, pHXB2 was amplified with SK38Δ, carrying a 18 base deletion (triangle) and SK39 (A). Subsequently, the first-round PCR product was re-amplified with SK38-SK39 primer pair. Second, a K1 fragment with 18 base deletion was generated using purified pSKAN and SK390 as primers (B). Finally, the competitor was made using SK380 and purified K1 as primers (C).

Quantitative of HIV-1 *gag* gene by competitive nested-PCR

Purification of nucleic acid

DNA of each lymphocyte subset was purified by using QIAamp DNA Blood Mini Kit (QIAGEN, Chatsworth, CA). Additional PBMCs from a HIV seronegative donor were added to a total of 2×10^6 cells if less than 2×10^6 cells were obtained. The PBMCs were resuspended in 200 µl of PBS, 20 µl of QIAGEN Protease and 200 µl of Buffer AL. The cell suspension was mixed by vortex for 15 sec and incubated at 56°C for 10 min. Two hundred microliters of ethanol was added to the mixture and mixed for 15 sec and applied to a QIAamp spin column that was placed in a collection tube, 500 µl of Buffer AW1 was added. The column was centrifuged at 12,000 rpm for 1 min and placed in a new collection tube, 500 µl Buffer AW2 was added in the column. The column was centrifuged at 12,000 rpm for 3 min. The solution in the collection column was discarded and the column was centrifuged at 12,000 rpm for 1 min again to remove all of the solution. The spin column was put in a 1.5 ml microcentrifuge tube. The DNA was eluted from the membrane by adding 200 µl Buffer AE, incubated for 5 min at room temperature and then centrifuged at 12,000 rpm for 1 min. The extracted DNA was stored at -20°C until used.

Quantitative competitive nested PCR assay

In competitive PCR, wild-type template was co-amplified with known amounts of competitive internal standard by using SK380/SK390 as outer primers and SK38/SK39 as inner primers (Table 4.). The PCR reaction was performed in a total volume of 50 µl. The first round PCR reaction, DNA template was subdivided in three parallel reaction (each reaction equal to 1.5×10^5 PBMCs) and each of reaction was co-amplified with increasing copy number of DNA competitor (25,50 and 100/5ul)

in PCR mixture (5 μl of 10x PCR buffer, 3 μl of 25 mM $MgCl_2$, 4 μl of 10 mM each of dNTP, 2 μl each of 10 pmol/μl SK380/SK390 primers, 0.3 μl of 5U/μl of Taq Polymerase enzyme deionized water to 50 μl. In every set of reaction, positive control (purified DNA from infected cell culture) and reagent blank were processed in parallel. PCR reaction tubes were run in a Thermal cycler 2400 or 9700 (Perkin-Elmer Cetus,CT,USA) at 95°C for 5 min and followed by 35 cycle: 95°C for 1 min, 60°C for 1 min and 72°C for 1 min. After 35 cycles, the reactions were run in 72°C for 7 min to complete extension then cooled at 4°. After the first round, 5 μl of primary PCR product was added to 45 μl of second round PCR reaction mixture which consisted of 5 μl of 10x PCR buffer, 3 μl of 25 mM $MgCl_2$, 4 μl of 10 mM each of dNTP, 2 μl each of 10 pmol/μl SK38/SK39 primers, 0.3 μl of 5U/μl of Taq Polymerase enzyme, and deionized water to 45 μl. The second round PCR cycle was performed under the same condition as the first round PCR cycle but the primer annealing temperature was changed from 60°C to 55°C.

Detection of amplified products by 10% polyacrylamide gel electrophoresis

PCR product from second round cPCR was run in 10% polyacrylamide gel. Ten milliliters of 10% gel was prepared by mixing 3 ml of 30.8% acrylamide stock (30% acrylamide and 0.8% Bis acrylamide, BioRad), 2ml of 5X TBE, 4.67 ml water, 30ul of 10% ammonium persulfate (Promega, WI, USA) and 3 μl TEMED (Promega, WI, USA). This solution was applied into space of vertical gel apparatus, added a comb and waited for gel polimerlization about 60 min. After gel polimerlization, 10 μl of PCR product and DNA marker (mixture of wild-type HIV-1 DNA and competitor DNA products) were mixed with 2 μl of 6X loading dye and loaded into a well of gel.

Electrophoresis was run in 0.5XTBE at 150 volts for 90 min in order to separate of the 115 bp wild-type DNA from the 97 bp competitor DNA product. Then the gel was stained with ethidium bromide and destained in water. The relative intensity in each lane of both DNA were measured from digital photograph and the peak areas (WA, wild-type area; DA, competitor area) of both amplified products were calculated by Gel-Pro analysis computer software. DA was corrected (DAc) for its lower molar ethidium bromide incorporation as follows: DAc = DA x (wild-type length/ competitor length) = DA x 1.185. The DAc/WA ratio was calculated for each lane and plotted against the copy number of competitor. Finally, the wild-type DNA copy was extrapolated from standard curve at ratio = 1.

Automated sequencing of *env* gene from PCR products

Polymerase chain reaction for V1V2 and V3 regions

The nested for V1/V2 region was generated with ENVB/AO2 as outer primers and AI1/AI2 as inner primers (Table 4.). The PCR reaction was performed in a total volume of 50 μl. The first round PCR reaction mixture consisted of 5 μl of 10x PCR buffer, 3 μl of 25 mM $MgCl_2$, 4 μl of 10 mM each of dNTP, 1 μl each of 10 pmol/μl ENVB/AO2 primers, 0.25 μl of 5U/μl of Taq Polymerase enzyme, 10 μl of DNA template and deionized water to 50 μl. In every set of reaction, positive control (purified DNA from cell culture positive) and reagent blank were processed in parallel. PCR reaction tubes were run in a Thermal cycler 2400 or 9700 at 95°C for 5 min and followed by 35 cycle of this sep: 95°C for 1 min, 50°C for 1 min and 72°C for 1 min. After 35 cycles, the reactions were run in 72°C for 7 min to complete extension then cooled at 4°. After 35 cycles, 5 μl of primary PCR product was added to 45 μl of

second round PCR reaction mixture which consisted of 5 µl of 10x PCR buffer, 3 µl of 25 mM MgCl$_2$, 4 ul of 10 mM each of dNTP, 1 ul each of 10 pmol/ul AI1-AI2 primers, 0.25µl of 5U/µl of Taq Polymerase enzyme, and deionized water to 45 µl. The second round PCR cycle was performed under the same condition as the first round PCR cycle but the primer annealing was changed from 50°C to 55°C.

The nested for V3 region was generated with AI1/AI2 as outer primers and CI1/BI2 as inner primers (Table 4.). The PCR reaction was performed in a total volume of 50 µl. The first round PCR reaction mixture consisted of 5 µl of 10x PCR buffer, 3 µl of 25 mM MgCl$_2$, 4 µl of 10 mM each of dNTP, 1 µl each of 10 pmol/µl AI1-AI2 primers, 0.25 µl of 5U/µl of Taq Polymerase enzyme, 10 µl of DNA template and deionized water to 50 µl. In every set of reaction, positive control (purified DNA from cell culture positive) and reagent blank were processed in parallel. PCR reaction tubes were run in a Thermal cycler 2400 or 9700 at 95°C for 5 min and followed by 35 cycle of this sep: 95°C for 1 min, 55°C for 1 min and 72°C for 1 min. After 35 cycles, the reactions were run in 72°C for 7 min to complete extension then cooled at 4°. After 35 cycles, 5 µl of primary PCR product was added to 45 µl of second round PCR reaction mixture which consisted of 5 µl of 10x PCR buffer, 3 µl of 25 mM MgCl$_2$, 4 ul of 10 mM each of dNTP, 1 ul each of 10 pmol/ul CI1-BI2 primers, 0.25µl of 5U/µl of Taq Polymerase enzyme, and deionized water to 45 µl. The second round PCR cycle was performed under the same condition as the first round PCR cycle.

Detection of amplified products by agarose gel electrophoresis

The amplified product from second round of nested PCR was detected by gel electrophoresis. All 50 microliters of product was mixed to 6X loading dye (see

appendix) and loaded into a well of 1.5% agarose gel (Pomega,USA). The 100 bp DNA ladder (NewEngland Biolab) was loaded in parallel. Electrophoresis was run in 0.5X Tris-Borate-EDTA buffer (TBE)(Amresco,Ohio,USA) at 100 volts until the loading dye migrated to the bottom of the gel. The gel was stained with 0.5 μg/ml of ethidium bromide solution for 7-10 min, followed by destaining in water for 10 min. The amplification bands were visualized by an UV transluminator (Spectronic, NY, USA) and photographed with a polaroid camera (Polaroid, MA, USA). The V1/V2, and V3 products were 1,300 bp and, 315 bp, respectively.

DNA purification by GENECLEAN II

PCR products of V1/V2, and V3 region from second round were run in 1.5 % agarose gel. After ethidium bromide staining, DNA was examined under UV light. The desired DNA band 1,300 and 315 bp was cut and put in 1.5 ml microcentrifuge tube and the gel was weighted. Three times volume of NaI solution was added into the tube and the mixture was incubated in 45°C- 55°C water bath for 5 min or until the gel was completely dissolved. Five microliter of GLASSMILK was added to the solution, mixed and incubated at room temperature for 5 min. In this step DNA was bound to the silica matrix. The tube was centrifuged at 12,000 rpm for 5 sec and the supernatant was discarded. Next, the pellet was washed two times with 10-50 volumes of NEW wash, centrifuged at 12,000 rpm for 5 sec and the supernatant was discarded. The DNA was eluted with TE pH8, incubated at room temperature for 5 min and centrifuged at 12,000 rpm for 1 min. Finally, the DNA in supernatant was placed in a new tube and kept at -20 °C until used.

Sequencing reaction

Sequencing reaction was performed in a total volume of 20 µl. Twenty nanograms of purified DNA were mixed with 4 µl of 0.8 pmol of PV1 and CI1 sequencing primers for V1V2 and V3 (see Table 4), 4 µl of Terminator Ready Reaction Mix and deionized water to 20 µl. The mixture was mixed well and centrifuged briefly. Next, the reaction tube was put in a thermal cycle and subjected to 25 cycles of 95 °C for 10 sec, 50 °C for 5 sec and 60 °C for 4 min and 4 °C until purified

. Purifying extension products by ethanol precipitation

The entire content of the extension reaction was added into 1.5 ml microcentrifuge tube containing 16 µl of deionized water and 64 µl of 95% ethanol. Then the tube was vortexed briefly and incubated at room temperature for 15 min to precipitate the extension product. After incubation the tube was centrifuge at 12,000 rpm for 20 min and the supernatant was carefully discarded. DNA pellet was washed with 250 µl of 75% ethanol, mixed by vortex briefly and centrifuged at 12,000 rpm for 10 min. The supernatant was carefully removed and DNA pellet was dried at 37 °C for 30 min.

Denaturing and loading sample

DNA pellet was resuspended in 25 µl of Template Suppression Reagent, vortexed briefly and spun down. Then the solution was transferred to sequencing tube and closed with septum. The sample was heated at 95 °C for 2 min to denature and chilled on ice for 2 min and load into the ABI Prism 310 Genetic Analyzer (Perkin-Elmer,USA).

Phylogenetic analysis of nucleotide sequences

Phylogenetic analysis was performed with DNASIS, ESEE3S and MEGA software. The nucleotide distance was calculated by Kimura's two parameters method. Phylogenetic tree was constructed using Neighbor-Joining method.

Statistic Analysis

The Mann-Whitney U test was used to analyzed differences between the amount of proviral DNA in different T-lymphocyte subsets that obtained from HIV-1 infected individuals with varied CD4 count. Correlation of CD4 count and proviral DNA were determined by using the Spearman correlation coefficient

CHAPTER V

Result

1. Clinical Statuses of subjects

All 30 HIV-1 infected persons (15 males and 15 females) did not have any risk behavior other than heterosexual. None of the patients received any anti-retroviral drug therapy. Patient characteristics were shown in Table 5. Twenty-two of 30 cases were asymptomatic, 5 cases had *M tuberculosis* infections, 1 case had Candidiasis, 1 case had *M scrofulaceum* infection, and the other case had herpes simplex infection. The age of the patients was 35±10 years, and their mean of CD4 counts was 201±163 cell/mm^3. There was no significant difference in CD4 counts between asymptomatic cases and cases complicated by TB and other infections.

Table 5. Characteristic of HIV-1 infected persons

NO	SEX	AGE	CD4 count	Rick factor	Sexual behavior	Clinical symptom
K1	F	31	192	Sexual	Heterosexual	Asymptomatic
K2	F	27	273	Sexual	Heterosexual	Asymptomatic
K3	F	34	316	Sexual	Heterosexual	Asymptomatic
K4	F	36	114	Sexual	Heterosexual	Oral Candidiasis
K5	F	21	307	Sexual	Heterosexual	Herpes simplex infection
K6	F	23	292	Sexual	Heterosexual	TB lymph node
K7	F	38	438	Sexual	Heterosexual	Asymptomatic
K8	M	44	406	Sexual	Heterosexual	Asymptomatic
K9	M	21	728	Sexual, IVDU	Heterosexual	Asymptomatic
K10	F	35	84	Sexual	Heterosexual	Asymptomatic
K11	F	31	291	Sexual	Heterosexual	Asymptomatic
K12	M	56	161	Sexual	Heterosexual	Asymptomatic
K13	M	53	230	Sexual	Heterosexual	Asymptomatic
K14	F	27	316	Sexual	Heterosexual	Asymptomatic
K15	M	40	106	Sexual	Heterosexual	Asymptomatic
K16	M	25	248	Sexual, IVDU	Heterosexual	Asymptomatic
K17	M	46	39	Sexual	Heterosexual	TB, Penicillosis
K18	M	26	25	Sexual	Heterosexual	Asymptomatic
K19	F	32	32	Sexual	Heterosexual	Asymptomatic
K20	M	49	55	Sexual	Heterosexual	Asymptomatic
K21	M	33	257	Sexual	Heterosexual	Asymptomatic
K22	M	29	19	Sexual	Heterosexual	Asymptomatic
K23	F	25	22	Sexual	Heterosexual	M scrofulaceum infection
K24	M	40	166	Sexual, IVDU	Heterosexual	Pulmonary TB
K25	F	27	15	Sexual	Heterosexual	TB pericarditis, TB lymph node
K26	F	23	350	Sexual	Heterosexual	Asymptomatic
K27	F	32	75	Sexual	Heterosexual	Asymptomatic
K28	M	52	294	Sexual	Heterosexual	Asymptomatic
K29	M	53	4	Sexual	Heterosexual	Asymptomatic
K30	M	34	177	Sexual, IVDU	Heterosexual	Pulmonary TB

2. CCR5 expression on CD4+ T cells in individual subjects.

Two-color flow cytometry was used to measures the expression of CCR5 on the CD4+ T cells, using specific monoclonal antibody directed against CCR5 and CD4. CCR5 expression was measured as the percentages of CD4+ T cells. The result showed that CCR5 expressed on CD4+ T cells range from 0.2 to 9.99%. In addition, there was a significant correlation between CCR5 expression of CD4+ T cells and CD4 counts, indicated that the patients with higher CD4 counts had more CD4CCR5+ cells. (r=0.462, p=0.01)

3. Isolation of CCR5+ and CCR5- T cells from PBMC.

PBMCs from 30 patients were isolated from fresh blood. Lymphocytes were separated by using a combination of a plastic adherent and immunomagnetic separation technique. The purity of cell separation were >95% and >85% of CCR5+ and CCR5-, respectively (Figure 6). After plating, monocytes contamination in lymphocytes (non adherent cells) were detected by staining non adherent cells with anti CD14-CD45, the result showed that there was only 1.4±1% monocyte contamination. After cell separating, 10 of 30 cases of CCR5-fraction were stained with anti CXCR4 to determine CXCR4 expression. CXCR4 was expressed on CCR5 negative cells ranged from 79 to 97% although this expression pattern was not correlated with CD4 count (r=0.28, p=0.44). This result suggested that most CCR5 negative T lymphocytes expressed CXCR4 receptor.

(A)

(B)

(C)

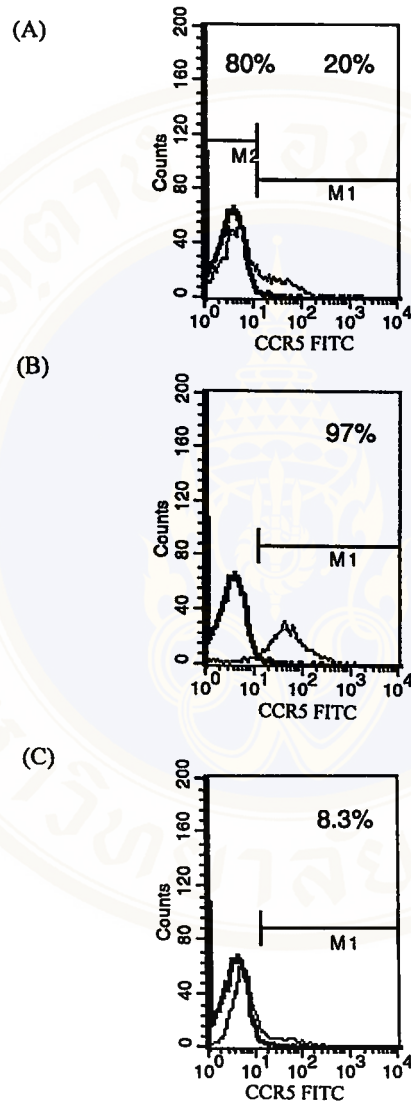**Figure 6.** Separation of T lymphocyte subsets. CCR5 expression on CD4+ T cells, thick line indicated negative control and thin line indicated unsorted CD4+ T cells (A). Purity of CCR5 positive fraction, thick line indicated negative control and thin line indicated CCR5 positive T cells (B). Purity of CCR5 negative fraction, thick line indicated negative control and thin line indicated CCR5 negative T cells (C).

4. Determination sensitivity of competitor

To determine the sensitivity of competitive nested PCR method by using end-point dilution amplification, the stock of DNA competitor (3×10^9 copies/μl) was 10-fold serial diluted from 10^{-1} to 10^{-11} and amplified for *gag* gene in duplicate by nested PCR with SK380/SK390 as outer primers, and SK38/SK39 as inner primers. The 97 bp fragment of amplified *gag* gene PCR product was directly detected on 2% agarose gel with ethidium bromide staining. The nested PCR could amplify the competitor DNA from undiluted below to the dilution of 10^{-9}. Thus, the sensitivity of nested PCR was at least 3 copies per reaction.

To verify the accuracy of competitor, the competitor was coamplified for *gag* gene with known amount of 8E5 cell that contains one copy of HIV-1 proviral DNA per cell. In this experiment, a constant copy number (10,000) of 8E5 was co-amplified, by using SK380/SK390 and SK38/SK39 as primers, with an increasing competitor copy number (300, 1,500, 3,000, 6,000 and 30,000). The result showed in Figure 7 that the lower band (97 bp) as competitor product competes with the upper band (115 bp) as 8E5 product. The graph shows the simple regression plotted by the intensity of competitor/wild-type ratio with the copy number of the competitor for each amplification tube. The copy number of 8E5 that calculated from the linear regression curve was 9,950 copies.

Figure 7. Optimization of competitor DNA
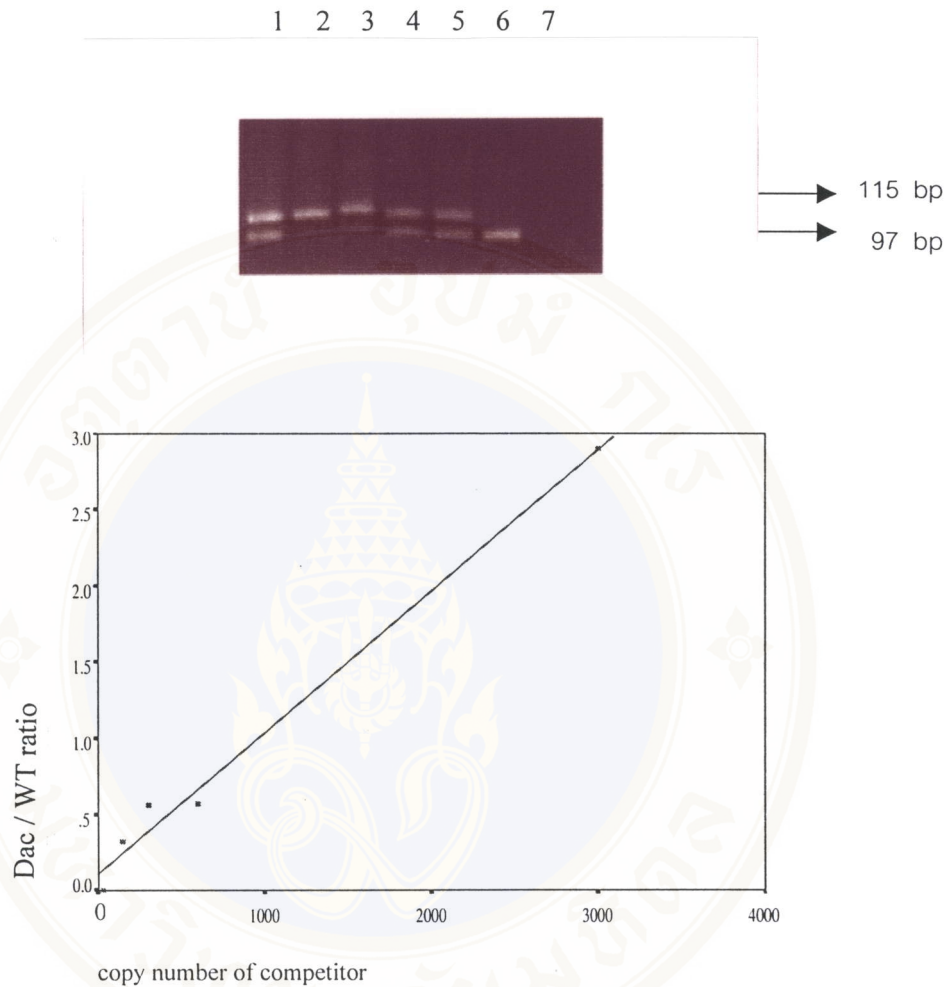
(A) Co-amplification of $1x10^4$ 8E5 copies (upper band, 115 bp) and the competitor (lower band, 97 bp). Lane 1 = marker, lane2 to 6; 300, 1500, 3000, 6000, 30000 copies of competitor, lane7= reagent blank, respectively.

(B) The linear regression curve plot between DAc/WA ratio and copy number of competitor. The amount of DNA was calculated by this curve equivalent to 9,550 copies.

5. Quantitation of HIV-1 proviral DNA in T-lymphocyte subsets

The amount of HIV-1 proviral DNA in CD4+ T-cells, CCR5+CD4+ T-cells, and CCR5-CD4+ T-cells was determined by using competitive nested PCR. In this assay, extracted DNA equivalent to 1.5×10^5 PBMCs of each fraction was co-amplified with 25, 50 and 100 copies of competitor DNA. Figure 8 shows quantitative of HIV-1 proviral DNA from unsorted cells of patient K18. The raw data of proviral DNA copy per 1.5×10^5 PBMCs was normalized to copies/10^5CD4+, CCR5+CD4+, and CCR5-CD4+ T-lymphocytes by using the percentages of CD4+ cells in each fraction of the same sample (Table6). The correlations of HIV-1 DNA copy number in each fraction and CD4 count were analyzed by Spearman correlation test.

5.1 HIV-1 proviral DNA in CD4+ T-lymphocyte

HIV-1 proviral DNA was detected in all 30 samples. The total proviral load had a broad range from 85 to 6,734 copies/10^5 CD4+ T cells (median = 389 copies/10^5 CD4+ T cells, Table6&8). The patients with low CD4 count had higher proviral DNA levels than patients with high CD4 count. There was inversely correlation between proviral DNA load and CD4 counts with Spearman's coefficients of -0.85, p = 0.01 (Figure 9). The patients with CD4 count more than 200 cells/mm^3 had a median of 184 DNA copies/10^5 CD4+ T cells (range, 85 to 916 copies/10^5 CD4+ T cells) and those with CD4 count lower than 200 cells/mm^3 had a median of 1,551 DNA copies/10^5 CD4+ T cells (range, 222 to 6,734 copies/10^5 CD4+ T cells). The HIV-1 proviral DNA differ significantly between patients with CD4 count more than 200 cells/mm^3 and patients with CD4 count less than 200 cells/mm^3 with p<0.01, Mann-Whitney U test (Figure 10).

Table 6. HIV-1 proviral DNA quantitation by competitive nested-PCR

No. of sample	CD4 Counts (cell/mm³)	Viral load (copies /1.5x10⁵ PBMCs)				Viral load (copies / 10⁵ CD4+cells)		
		CD4+	CCR5- CD4+	CCR5+ CD4+	Monocyte	CD4+	CCR5- CD4+	CCR5+ CD4+
K29	4	100	95	39	-*	6734	4311	3650
K25	15	95	90	36	-*	6345	5089	3921
K22	19	97	82	33	Neg	4974	4975	1330
K23	22	101	83	112	Neg	2047	5157	1495
K18	25	101	80	9	Neg	2584	2252	201
K19	32	59	52	50	Neg	2129	2042	825
K17	39	55	50	42	-*	1222	847	1278
K20	55	78	69	87	Pos<25	2083	1864	1897
K27	75	58	48	57	-*	678	735	569
K10	84	30	32	53	Pos<25	361	283	669
K15	106	119	182	174	-*	1277	1249	852
K4	114	170	147	316	Neg	1825	800	2700
K12	161	22	34	47	Neg	523	817	951
K24	166	33	30	81	-*	318	158	1627
K30	177	35	34	44	-*	222	149	410
K1	192	25	39	164	Neg	704	310	1700
K13	230	12	12	19	Pos<25	117	73	246
K16	248	27	88	131	-*	103	249	1471
K21	257	35	37	53	Pos<25	292	164	709
K2	273	64	77	63	Neg	916	1341	654
K11	291	43	40	69	-*	201	57	322
K6	292	41	41	105	Pos<25	183	144	357
K28	294	45	40	60	-*	264	202	405
K5	307	29	23	43	Pos<25	184	94	408
K14	316	50	50	126	-*	170	39	873
K3	316	42	48	232	Neg	416	634	850
K26	350	57	50	22	-*	294	140	705
K8	406	23	24	111	-*	88	35	689
K7	438	35	45	102	-*	162	47	1508
K9	728	39	19	80	-*	85	24	1110

-* not done

Neg = negative

Pos = positive

Table 7. HIV-1 proviral DNA quantitation by competitive nested-PCR and the predicted viral phenotype based on V1-V3 sequence

No. of sample	CD4 counts (cell/mm³)	Viral load (copies / 10⁵ CD4+cells)			CCR5+ CD4+/ CCR5-CD4+ ratio	Viral phenotype
		CD4+	CCR5- CD4+	CCR5+ CD4+		
K29	4	6734	4311	3650	0.85	NSI
K25	15	6345	5089	3921	0.77	SI
K22	19	4974	4975	1330	0.27	SI
K23	22	2047	5157	1495	0.29	NSI
K18	25	2584	2252	201	0.09	NSI
K19	32	2129	2042	825	0.4	NSI
K17	39	1222	847	1278	1.51	NSI
K20	55	2083	1864	1897	1.02	NSI
K27	75	678	735	569	0.77	SI
K10	84	361	283	669	2.36	SI
K15	106	1277	1249	852	0.68	SI
K4	114	1825	800	2700	3.38	SI
K12	161	523	817	951	1.15	SI
K24	166	318	158	1627	10.29	-*
K30	177	222	149	410	2.75	NSI
K1	192	704	310	1700	5.78	NSI
K13	230	117	73	246	3.37	SI
K16	248	103	249	1471	5.91	NSI
K21	257	292	164	709	4.32	SI
K2	273	916	1341	654	0.49	SI
K11	291	201	57	322	5.91	NSI
K6	292	183	144	357	2.48	NSI
K28	294	264	202	405	2	-*
K5	307	184	94	408	4.34	NSI
K14	316	170	39	873	22.38	NSI
K3	316	416	634	850	1.34	NSI
K26	350	294	140	705	5.04	NSI
K8	406	88	35	689	19.69	NSI
K7	438	162	47	1508	32.08	NSI
K9	728	85	24	1110	46.25	NSI

-* unable to be amplified

Table 8. HIV-1 proviral DNA copy number in T lymphocyte subsets and ratio of

HIV-DNA in CCR5+CD4+ and CCR5-CD4+ T lymphocytes

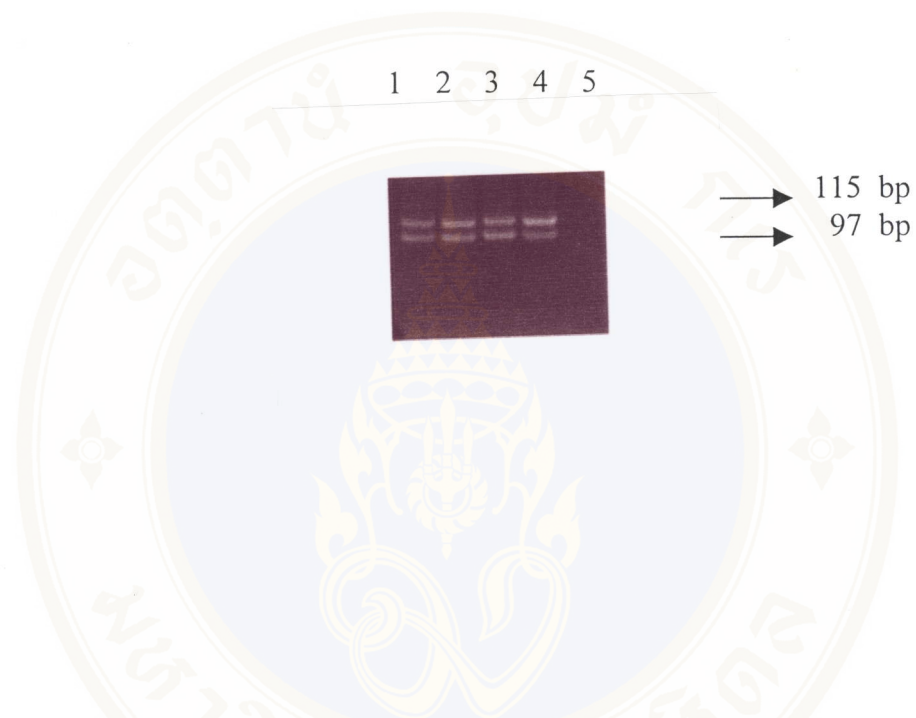| T lymphocyte subsets	Proviral DNA (copies/10^5 CD4+ T cells)	
	Median	Range
Unsorted CD4+ T cell	389	85-6,734
CCR5-CD4+ T cells	297	24-5,157
CCR5+CD4+ T cells	851	201-3,921
CCR5+CD4+/CCR5-CD4+ Ratio	2.42	0.09-46.25

Figure 8. Quantitative of HIV-1 proviral DNA by competitive nested-PCR

Co-amplification of 1.5×10^5 PBMCs (upper band, 115 bp) and the competitor

(lower band, 97 bp).   Lane 1 = marker, lane2 to 4; 100, 50, 25 copies of

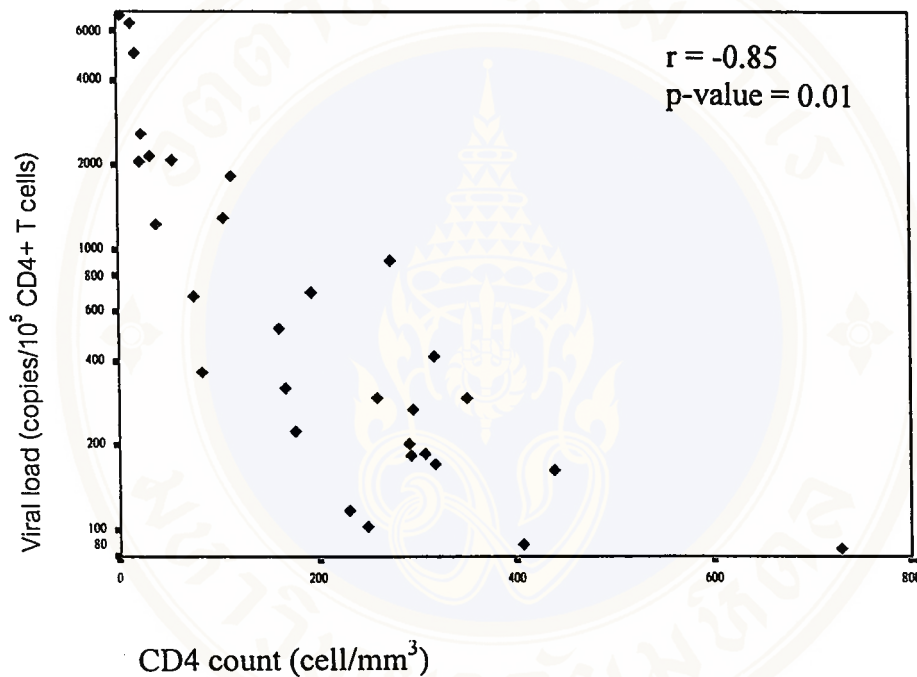competitor, lane5= reagent blank, respectively.

Figure 9. Scatter plot between CD4 count and HIV-1 proviral DNA copy number in unsorted CD4 T-cells. The HIV-1 DNA copy number were measured in unsorted non-adherent PBMCs, and the copy number/10^5 CD4+ cells were calculated using % CD4 in lymphocyte population. The Spearman correlation coefficient (r) and P-value were shown.
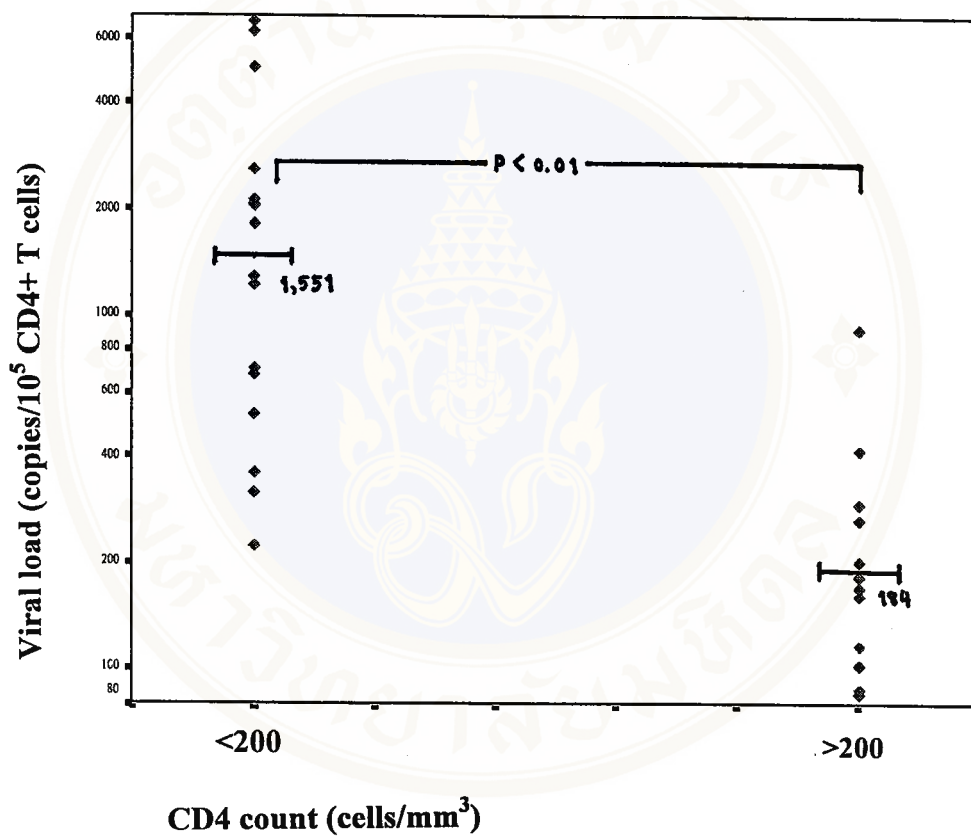
Figure 10. HIV-1 proviral load in unsorted CD4+ T cells is shown for individuals with CD4 count less than 200 cell/mm³ and individuals with CD4 count more than 200 cell/mm³. The number and bars in the graph indicated median values. The P-value of Mann-Whitney U test was shown.

5.2 HIV-1 proviral DNA in CCR5+CD4+ and CCR5-CD4+ T-lymphocyte subsets

HIV-1 proviral DNA was detected in both CCR5+CD4+ and CCR5-CD4+ T-lymphocyte subsets in all patients (Table6&8).   The amount of proviral DNA in CCR5+CD4+ T-lymphocytes had a broad range from 201 to 3,921 copies/10^5 CD_4^+ T cells (median = 851 copies/10^5 CD_4^+ T cells). No correlation was found between CD4 count and proviral DNA in CCR5+CD4+ T-lymphocyte (r = -0.33, p = 0.072) (Figure 11). The patients with CD4 count more than 200 cells/mm^3 had a median of 697 DNA copies/10^5 CD4+ T cells (range, 246 to 1,508 copies/10^5 CD4+ T cells) and those with CD4 count lower than 200 cells/mm^3 had a median of 1,304 DNA copies/10^5 CD4+ T cells (range, 201 to 3,921 copies/10^5 CD4+ T cells). The HIV-1 proviral DNA differ significantly between patients with CD4 count more than 200 cells/mm^3 and patients with CD4 count less than 200 cells/mm^3 with p=0.02, Mann-Whitney U test (Figure 12).

The amount of proviral DNA in CCR5-CD4+ T-lymphocytes had a broad range from 24 to 5,157 copies/10^5 CD_4^+ T cells (median = 297 copies/10^5 CD_4^+ T cells). There was an inversely correlation between CD4 count and proviral DNA in CCR5-CD4+ T-lymphocyte (r = -0.87, p<0.01)(Figure 13). The patients with CD4 count more than 200 cells/mm^3 had a median of 117 DNA copies/10^5 CD4+ T cells (range, 24 to 1,341 copies/10^5 CD4+ T cells) and those with CD4 count lower than 200 cells/mm^3 had a median of 1,048 DNA copies/10^5 CD4+ T cells (range, 149 to 5,157 copies/10^5 CD4+ T cells).   The HIV-1 proviral DNA differ significantly between patients with CD4 count more than 200 cells/mm^3 and patients with CD4 count less than 200 cells/mm^3 with p<0.01, Mann-Whitney U test (Figure 14).

When comparing the amount of proviral DNA in CCR5+CD4+ and CCR5-CD4+ T lymphocyte subsets, we found that the ratio of proviral DNA in CCR5+ and CCR5-CD4+ T cells was 0.09- to 46.3-fold (median = 2-fold, Table7&8). This CCR5+CD4+ load/ CCR5-CD4+ load ratio correlated with CD4 count ($r = 0.76$, $p < 0.01$ Figure 15). Low ratio were found in patient with CD4 count <200 cells/mm^3 (median = 0.93-fold), whereas high ratio were found in patient with CD4 count >200 cells/mm^3 (median = 4.69-fold). The CCR5+CD4+ load/ CCR5-CD4+ load ratio in patient with CD4 count <200 cells/mm^3 were significant less than CCR5+CD4+ load/ CCR5-CD4+ load ratio in patient with CD4 count >200 cells/mm^3 ($p=0.02$, Mann-Whitney U test, Figure16)

5.3 Quantification of HIV-1 proviral DNA in monocytes

HIV-1 proviral DNA in monocytes were detected in 15 of 30 cases (Table 6). The HIV-1 positive by nested PCR were 6 from 15 cases (40%). The copy number of HIV-1 proviral DNA in monocytes of 6 HIV-1 positive cases were measured. Amount of proviral DNA of K5 less than 25 copies/4.37×10^4cells, K6 less than 25 copies/1.12×10^4cells, K10 less than 25 copies/2.2×10^4cells, K13 less than 25 copies/1.5×10^4cells, K20 less than 25 copies/1×10^4cells, and K21 less than 25 copies/1.1×10^4cells.

Figure 11. Scatter plot between CD4 count and HIV-1 proviral DNA copy number in CCR5+CD4 T-cells. The HIV-1 DNA copy number were measured in CCR5 positive non-adherent PBMCs, and the copy number/10^5 CD4+ cells were calculated using % CCR5CD4 in lymphocyte population. The Spearman correlation coefficient (r) and P-value were shown.

Figure 12. HIV-1 proviral load in CCR5+CD4 T cells is shown for individuals with CD4 count less than 200 cell/mm^3 and individuals with CD4 count more than 200 cell/mm^3. The number and bars in the graph indicated median values. The P-value of Mann-Whitney U test was shown.
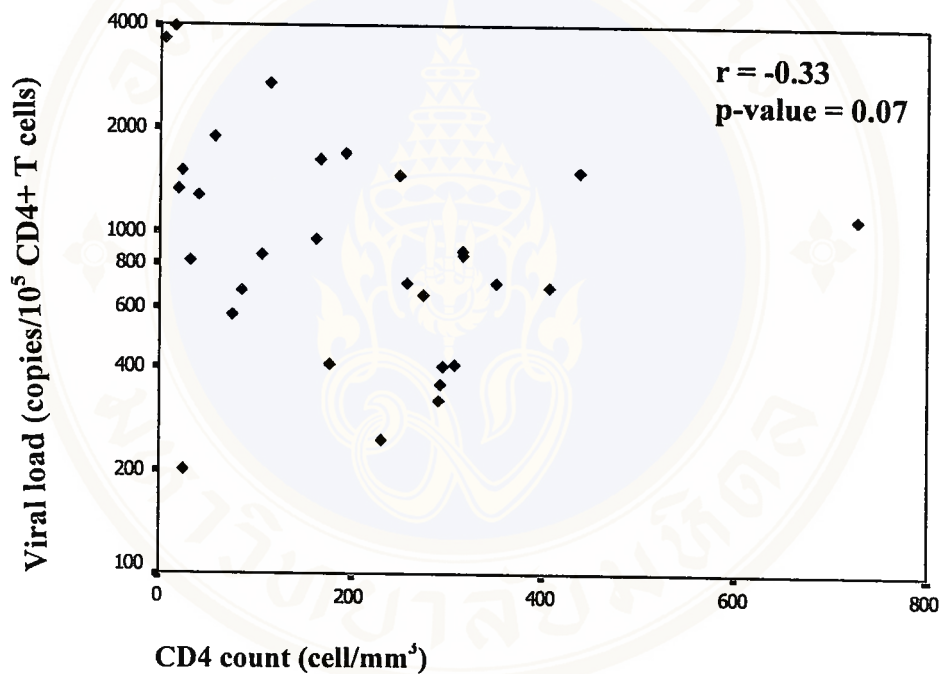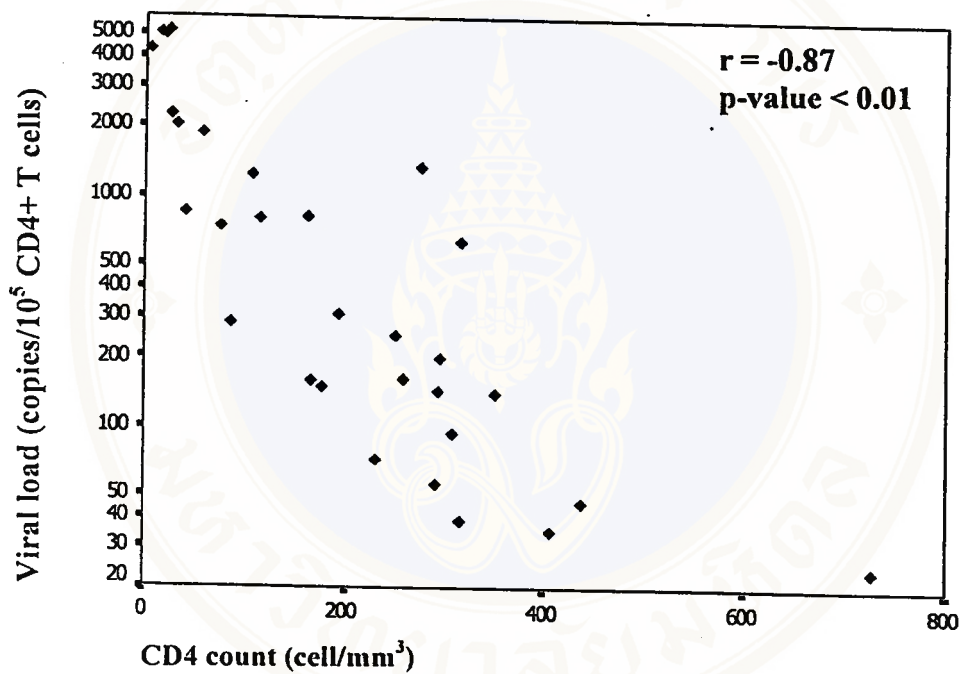
Figure 13. Scatter plot between CD4 count and HIV-1 proviral DNA copy number in CCR5-CD4 T-cells. The HIV-1 DNA copy number were measured in CCR5 negative non-adherent PBMCs, and the copy number/10^5 CD4+ cells were calculated using % CCR5CD4 in lymphocyte population. The Spearman correlation coefficient (r) and P-value were shown.
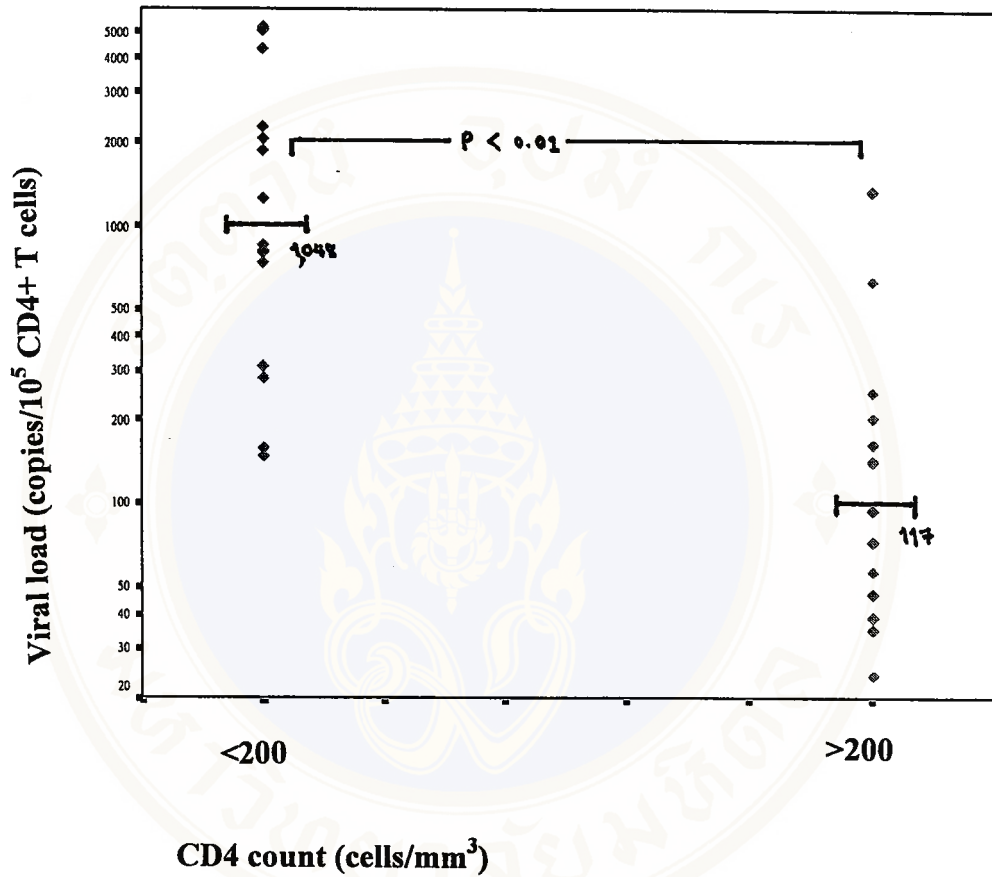
Figure 14. HIV-1 proviral load in CCR5-CD4+ T cells is shown for individuals with CD4 count less than 200 cell/mm^3 and individuals with CD4 count more than 200 cell/mm^3. The number and bars in the graph indicated median values. The P-value of Mann-Whitney U test was shown.

Figure 15. Scatter plot between CD4 count and the ratio of HIV-1 proviral DNA

in CCR5+CD4+ and CCR5-CD4+ T cells. The Spearman correlation coefficient

(r) and P-value were shown.

Figure 16. Ratio of proviral load in CCR5+CD4+ and CCR5-CD4+ T cells. The ratio between the frequency of proviral DNA in CCR5+CD4+ an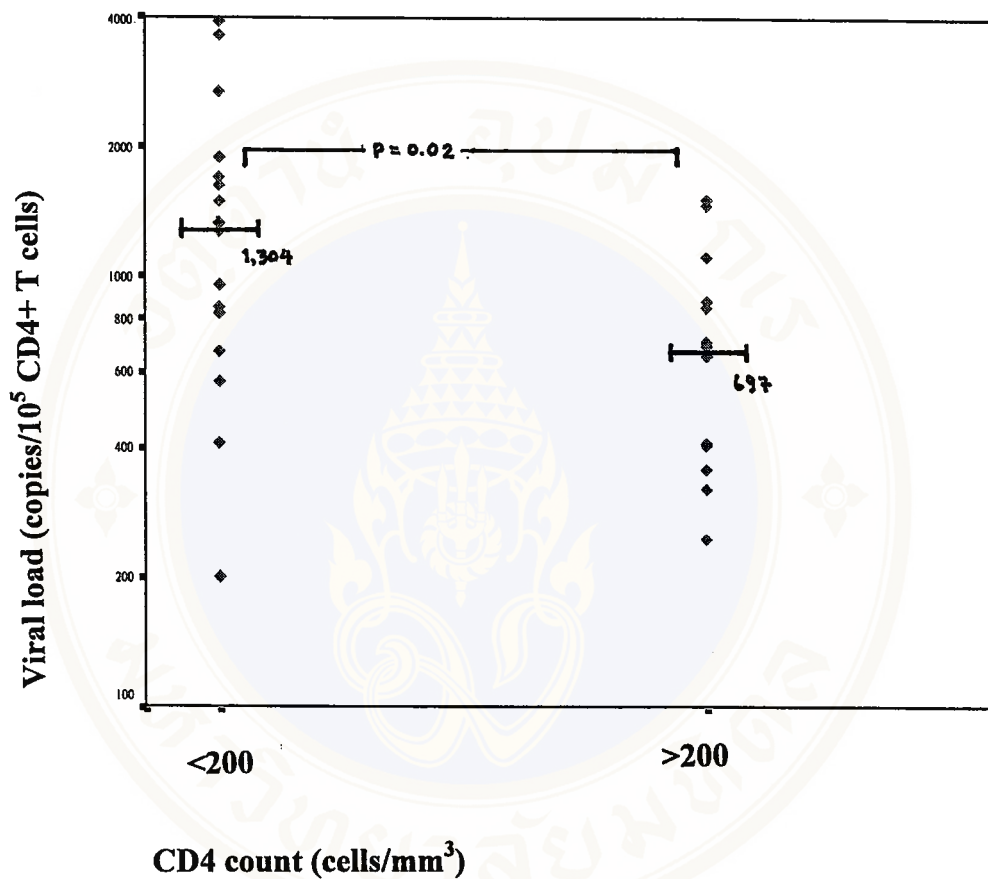d proviral DNA in CCR5-CD4+ T cells is shown for individuals with CD4 count less than 200 cell/mm³ and individuals with CD4 count more than 200 cell/mm³. The number and bars in the graph indicated median values. The P-value of Mann-Whitney U test was shown.
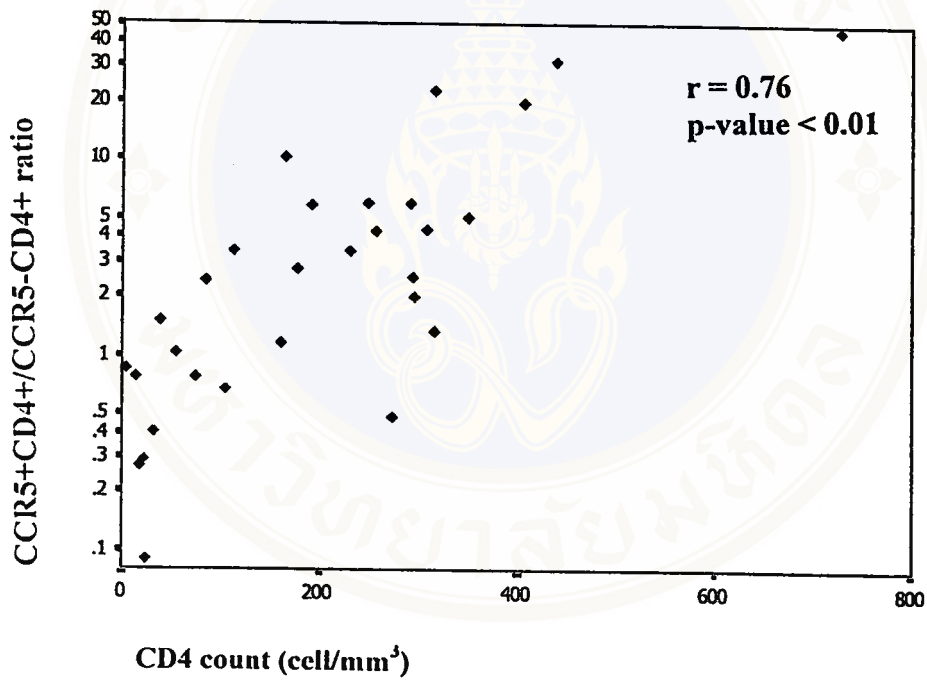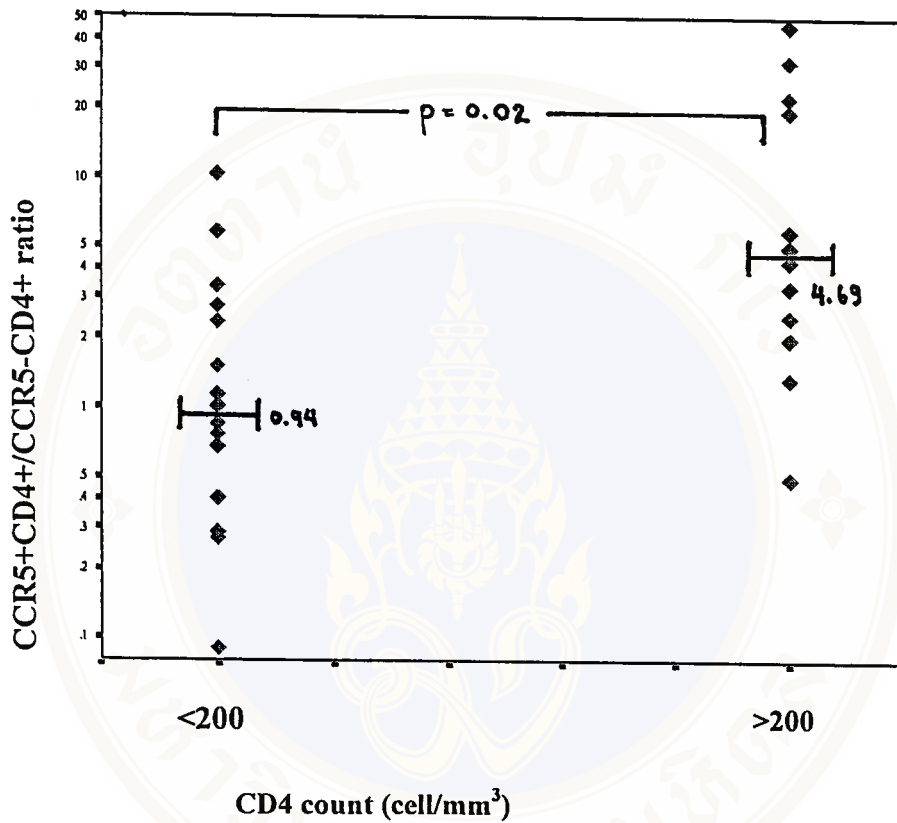
6. Nucleotide sequencing of HIV-1 V1, V2, and V3 region in *env* gene

To predict HIV-1 phenotype in blood samples, nucleotide sequencing of V1/V2 region was performed in 12 patients and V3 region was performed in 28 patients. The PCR products of V1V2 and V3 regions were directly sequenced with sequencing primers, fluorescent dye terminator, and automated sequencer as described in materials and methods. The nucleotide and amino acid sequence multiple alignments were performed with DNASIS version 2.1. The phylogenetic analysis was performed by ESEE and MEGA software. The phylogenetic tree was constructed by using Neighbor-Joining method.

6.1 V3 loop sequences

The predicted amino acid sequence alignments in individual patients at the V3 regions were shown in Figure17 and the consensus nucleotide and amino acid of all sequences was shown at the top of figure. In addition, their phylogenetic tree with the nucleotide sequences of these samples was also shown in Figure18. All of V3 nucleotide sequences in this study were grouped as subtype E. The distances of nucleotide sequences of the V3 region was 12 ±4.9%.

Specific amino acid variation in the V3 loop can be used as markers to predict HIV-1 viral phenotype. In this study, the viral phenotype (NSI and SI) was predicted with V3 amino acid sequences by using 4 criterias (67). First, a positive charged or basic amino acid (arginine or lysine) at position 11, 13 or 25 in V3 correlates with SI viruses, where as NSI viruses correlate with uncharged or negative charged amino acid at these positions. Second, the conserved N-linked glycosylation site in V3 (NXT/S, amino acid at position 6,7,8) is indicated NSI viruses, while the lost N-linked glycosylation site and the substitution of a basic amino acid (arginine; R)

at position 8 is required for SI viruses. Third, the net charges of amino acid, five or more than five are indicated SI viruses, while less than 5 are indicated NSI viruses. Finally, the SI viruses contain GPGR or GPGH V3 motif instead of GPGQ.

By these methods, 10 (35.7%) of 28 cases were predicted to be SI and 18 (64.3%) NSI viruses (Table 9). One of 10 predicted SI virus (K4) had a positively charged amino acid (R) at position 11 and a negatively charged amino acid (E) at position 25,with the net charged amino acid of +5 and contained GPGR motif. Five of 10 predicted SI viruses: K2, K15, K21, K25, and K27 had positive charged amino acids (R) at position 13, a negatively charged (D) or uncharged (N or G) at position 25. All of them had GPGQ motif, with the net positively charged of 4, except K27 had 5 net positively charged. Three of 10 predicted SI viruses: K10, K12, and K13 had uncharged amino acids (G or S) at position 11, a negatively charged (E) or uncharged (N or A) at position 25. All of them had GPGR motif, with the net positively charged more than 4, except K10. The other one of predicted SI virus had GPGH motif, with the net charged of 4 and contained uncharged (G) and negatively charged (E) at position 11 and 25, respectively. The V3 sequence from 23 predicted NSI viruses contained uncharged amino acid (G or S) at position 11 and negatively charged (E or D) or uncharged (G or N) at position 25. The net charged of all predicted NSI viruses less than 5, except K27, that was +5. All of predicted NSI viruses had GPGQ motif and conserve N-glycosylation site.

We also sequence the V3 region of CCR5+ and CCR5- T lymphocyte of the same patient (K7,K10,K12). The nucleotide sequences and their predicted phenotype of all patients that derived from CCR5+ T cells were closely related with nucleotide sequences that derived from CCR- T cells (Figure 18).

Table 9. Characteristics of V3 loop sequences of predicted SI and NSI phenotypes

No of Sample	V3					Predicted Phenotype
	Positive charge of amino acid at position		V3 motif	N-link glycosylation site	Net charge	
	11 or 25	11,13 or 25		N-X-S/T		
23	0	0	GPGQ	0	≤4	NSI
10	1	6	GPGR,GPGH ,GPGQ	0	4, ≥5	SI

```
                              10        20        30        40
TH253.AMI   1 CTRPSNNTRT SIPIGPGQA- FYRTGDIIGD IRKAYC....
K1.AMI      1 ....F..... ..H.....V- L.K......N ..Q.......
K2.AMI      1 .......... ..R.....V- ..G..N.... ..R.......
K3.AMI      1 .......... .MT.....V- W......T.. ....F.....
K4.AMI      1 .......VKK R.TM...RV- Y.S.KE.V.. ..S... ...
K5.AMI      1 ....F..... ..T.....V- .......... ..R.......
K6.AMI      1 .........Q ..N.....ML .......... ..Q.......
K7.AMI      1 .....T.... ..H.....V- .......T.. ....N.....
K8.AMI      1 .........K ..T.....VL .......... ..G.......
K9.AMI      1 .......... .LT.....V- .......T.. ..........
K10.AMI     1 .......... G.TM...RV- .....EL... ..........
K11.AMI     1 .......... G.T.....V- .....E.V.. ..Q.......
K12.AMI     1 .........R ..T....RV- ...---.N.... 
K13.AMI     1 .......I.V .MT....RV- .....A.T.. ..........
K14.AMI     1 .......... ..T.....V- .........E ..........
K15.AMI     1 .......... ..R.....V- .........N P.I.......
K16.AMI     1 .......... ..N.....V- .......... ..........
K17.AMI     1 .......... ..T.....V- ..I......E ..........
K18.AMI     1 .........R .AT.....VL ...P..V... ..Q.......
K19.AMI     1 .......... .MT.....V- .......... ..........
K20.AMI     1 .......I.K .LTV....V- L......... ..........
K21.AMI     1 .......... ..R.....V- .......A.. ..........
K22.AMI     1 .......... G.TM...HV- .....E.... ..........
K23.AMI     1 .....T.... ........V- .......T.. ..Q.......
K25.AMI     1 .......... ..R......- ..K....T.. ..R.F.....
K26.AMI     1 .......... GVHM....V- .......... ..........
K27.AMI     1 ......QI.A .LR.....V- ..K.EG.G.N ..R.F.....
K29.AMI     1 .......... .TS....A.- .......... ..Q.F.....
K30.AMI     1 ....Y..... .LN.....V- .......... ..P.T.....
```

Figure 17. Alignment of predicted amino acid sequences of the V3 region of 28 HIV-1 infected persons. The consensus sequence was shown at the top of figure. The number above the sequenced indicated the position of amino acid. The amino acids different from the consensus sequence were shown. The amino acid similarity and deletion were indicated by dot and dash, respectively. The potential N-linked glycosylation site (NXS/T) was underlined.

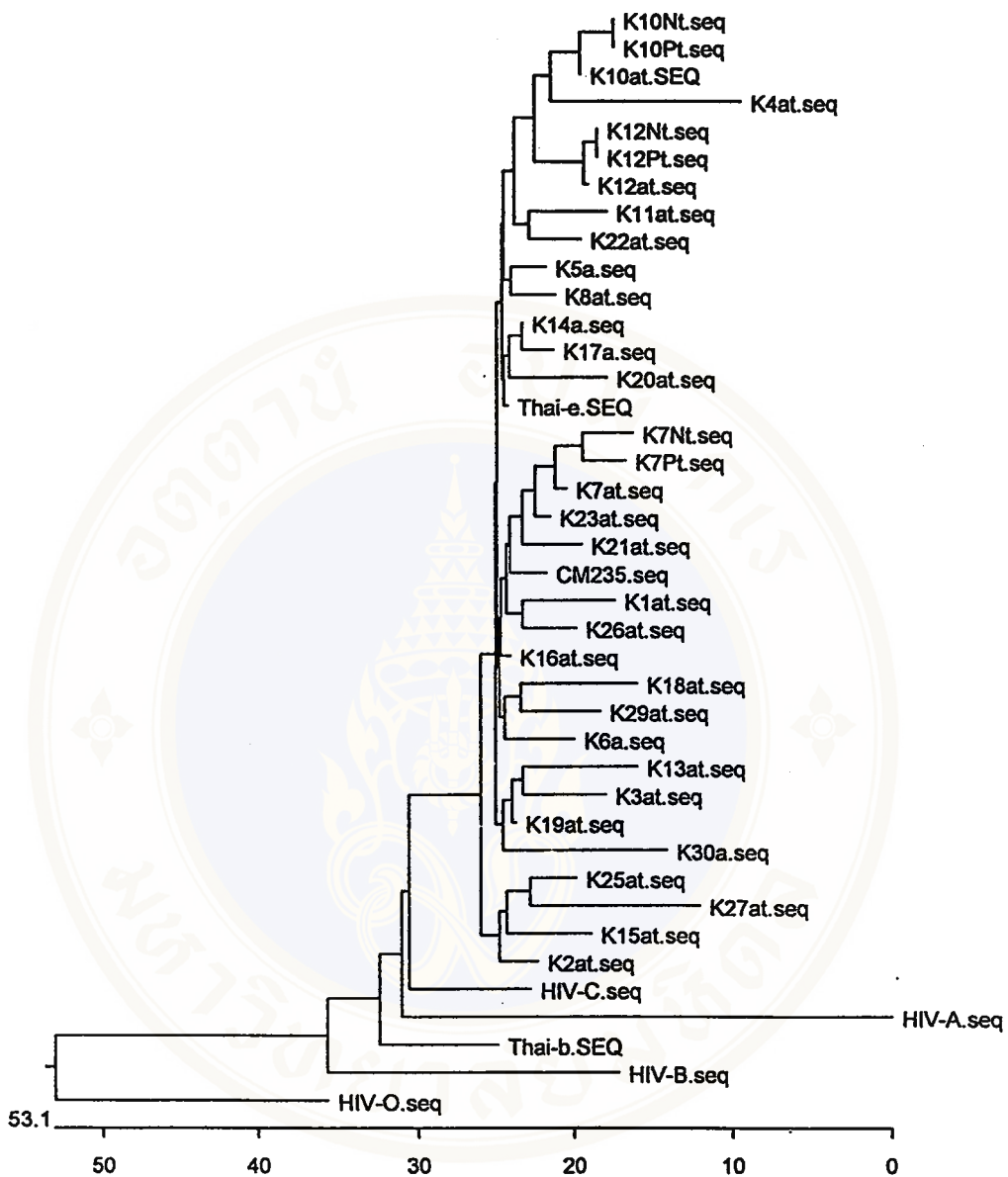**Figure 18.** Phylogenetic analysis of HIV-1 V3 region of 28 HIV-1 infected

persons. Tree was constructed by using Neighbor Joining method. The reference

subtypes were included, which letter A, B, C, and O referred to HIV-1 subtypes.

The scale bar represented the percentage of nucleotide sequence divergence. The

tree was unrooted and branch length was proportional to the number of nucleotide

change.

6.2 V1 and V2 sequences

The V1V2 region in 12 cases was sequences to predict the viral phenotype. Previous reports the V1V2 region contained the major determinants of SI capacity. The long V2 and increasing of N-glycosylation site in V2 correlate with SI virus (70).

The predicted amino acid sequence alignments of the V1V2 region were performed in 5 V3-predicted SI viruses and 7 V3predicted NSI viruses and shown in Figure19. Sequence analysis showed that there were deletion, insertion, and substitution of amino acids in V1 and V2 regions. The length of the V1 segment from predicted SI viruses ranged from 32 to 41 amino acids, with a mean of 35 amino acids, while the V1 segment from predicted NSI viruses varied between 28 and 34 amino acids, with a mean of 26 amino acids. The length of the V2 segment from predicted SI viruses ranged from 38 to 44 amino acids, with a mean of 41 amino acids, while the V2 segment from predicted NSI viruses varied between 40 and 42 amino acids, with a mean of 41 amino acids. Although, the length of the V1 segment of predicted SI viruses longer than predicted NSI viruses, with p value = 0.05 Mann-Whitney U test. No difference was found between the length of V2 of predicted SI and NSI viruses (p=0.55). The number of positively charged amino acid in V2 region ranged from 3 to 6 (mean, 5.2) in predicted SI viruses and from 4 to 7 (mean, 5.6) in predicted NSI viruses. Thus, no difference in the number of positive charged amino acid in V2 region of predicted SI and NSI viruses (p=0.64). We also examined the changes in the N-glycosylation site of the V1 and V2 regions, there were no difference in the number of N-glycosylation site in the V1 and V2 regions between both groups with the same p value = 0.88.

```
                 10         20         30         40         50         60         70         80        90
TH253.AMI      1 CVTLNCTNA- NLTN--VDNI T----NGSNI IG-NITDEVR NCSFNMTTEL RDKKQKVHAL FYKLDIVQIE DNS-S--SEY RLINC.....
K2V1V2.AMI     1 ......SI   TVN.TSYVD. .----DEA-- -TGD...DEG ....I      I I.N.KEAY. .Y.VV.PLD  E.D----GI. ..........
K4V1V2.AMI     1 ....H.N.KI .V.DRTT... .-----VPG. .-....M.   ....V  T.. .......... .........  D N.EN.---. ..........
K7V1V2.AMI     1 ....H....V ----FRNTT. .----.TDR  .-...N.... .......... .......AY. .......G   .SG----.D  ..........
K8V1V2.AMI     1 ....F..    ---.WTNVY. .----TDAYN VS--VP.... ...T....T. I.MTP.Q..  ...VHA.FS. NDIVP--T.. ..........
K10V1V2.AMI    1 ....E.AE.K GANDTNTAYD .YRNCDMMLT VIG.R.YDMT T.T....P.V L.LMH....  L.E....D   SD------... ...R......
K11V1V2.AMI    1 .......... K..F--.    N---...T.. L.GDAA.G.  S......... ..KQLP...  .L.VML.V.  E.NS.--G.. ..........
K12V1V2.AMI    1 .......... ...FTKA.V  .----TTT.A SE-DMKE.G  .T.T....T. ..K.Q....Y ..I..H.T   NS------... ..........
K14V1V2.AMI    1 .......... K-------.  .----.DP-. L.-....K   ....I..... .........  ...M...    .TN------.. ..........
K18V1V2.AMI    1 .......... T.....-A   .----.TTA. --G.TAE.T  ..YI INT.L.Q.  .Q.VFYKMN  VS.T----.G .I.D......
K19V1V2.AMI    1 ...I.....  ---.LHNTTRV ----.A.I.  G--.V..D.. ........K.R..Y...  PP..G.GNN--GK. ..........
K25V1V2.AMI    1 ......STTL T---WNGTTD G----PNRD. .-......G  .........D. K.......Y. ..........G SSNN.NY.D. ..........
K26V1V2.AMI    1 ....D..D.N LTQANNASDV S-------S  .AGDVS.CLG .MTYEL.DGI INVTAMI..  NH..A.HNG  RD------... ...Q......
```

Figure 19. Alignment of predicted amino acid sequences of the V1V2 region of 12 HIV-1 infected persons. The consensus sequence was shown at the top of figure. The number above the sequenced indicated the position of amino acid. The amino acids different from the consensus sequence were shown. The amino acid similarity and deletion were indicated by dot and dash, respectively. The potential N-linked glycosylation site (NXS/T) was underlined.

7. Correlation between predicted viral phenotype and the ratio of proviral DNA in CCR5+CD4+ and CCR5-CD4+ T cells

In this study, we also compared the amount of proviral DNA in CCR5+CD4+ and CCR5-CD4+ T lymphocyte subset obtained from 10 V3-predicted SI and 18 V3-NSI individuals. The result showed that, the ratio of proviral DNA in CCR5+CD4+ and CCR5-CD4+ T cell subset in individuals with predicted SI virus ranged from 0.27- and 4.32-fold with a median of 0.96-fold, this CCR5+CD4+ load/ CCR5-CD4+ load ratio not correlated with CD4 count ($r = 0.37$, $p = 0.29$). The ratio of CCR5+CD4+ load and CCR5-CD4+ load in individuals with predicted NSI virus varied from 0.09- to 46.25-fold with a median of 3.55-fold, this CCR5+CD4+ load/ CCR5-CD4+ load ratio correlated with CD4 count ($r = 0.83$, $p < 0.01$). Thus the median ratio of CCR5+CD4+ load and CCR5-CD4+ load in predicted SI individuals was significantly lower than the median ratio in predicted NSI individuals, with $p=0.07$, Mann-Whitney U test (Figure 20). However, among those samples with low HIV-DNA in CCR5+CD4+/ CCR5-CD4+ ratio, about only half of them showed SI predicted phenotype (4 out of 9 samples with ratio <1 and 10 out of 20 with ratio < 5). Infact, the sample with the lowest ratio (K18) had predicted NSI phenotype. We found some patients who were infected by predicted NSI virus had low level of proviral DNA load ratio and low CD4 count.
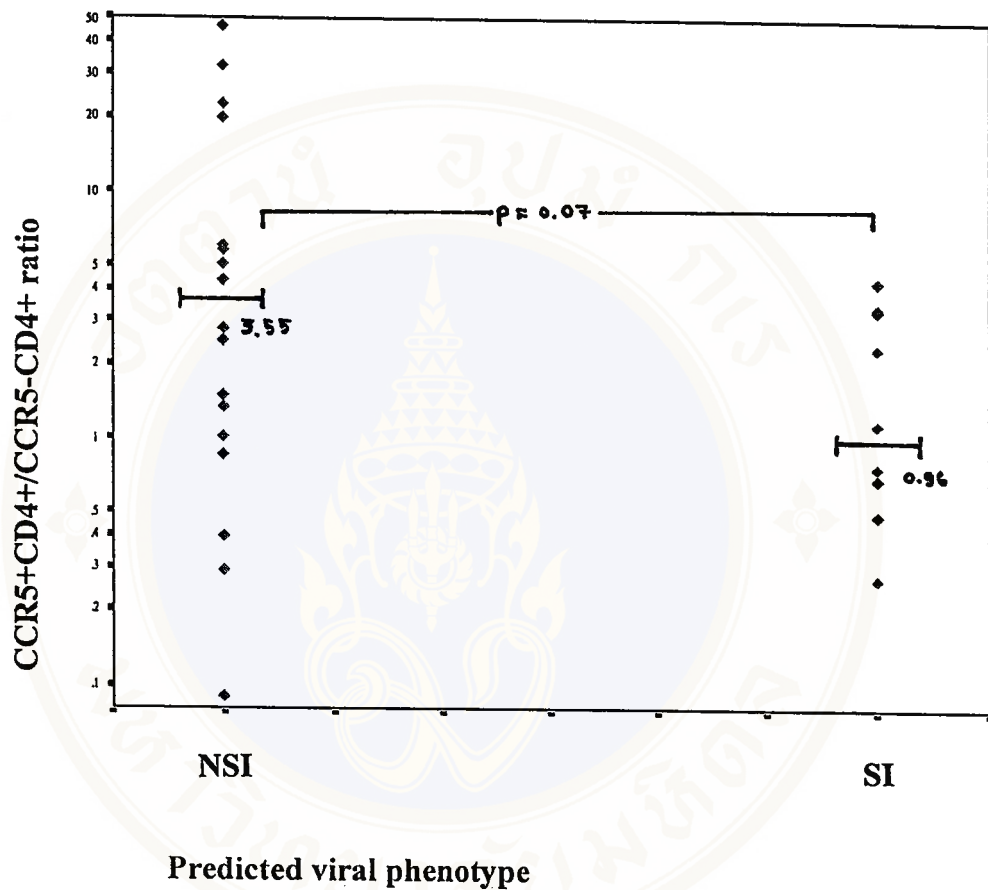
Figure 20. Ratio of proviral load in CCR5+CD4+ and CCR5-CD4+ T cells. The ratio between the frequency of proviral DNA in CCR5+CD4+ and proviral DNA in CCR5-CD4+ T cells is shown for individuals with predicted NSI and SI virus strains. The number and bars in the graph indicated median values. The P-value of Mann-Whitney U test was shown.

CHAPTER VI

DISCUSSION

HIV-1 infection requires the CD4 and the chemokine receptor for viral entry and also requires cellular activation for the viral replication and protein expression. The major HIV-1 chemokine receptor, CCR5 and CXCR4 receptors, have been shown to be differentially expressed in CD4+ T lymphocyte subpopulations. CCR5 is predominately expresses in CD45RO+ memory T cells, while CXCR4 is predominately expresses in CD45RA+ naive T cells (12-14). This differential expression of both HIV-1 coreceptor suggests that different T cell subsets will differ in susceptibility to viruses of various phenotypes (CCR5-using and CXCR4-using viruses).

In this study, the amount of HIV-1 proviral DNA in different CD4+ T cell subsets were measured by using competitive nested PCR. At present, competitive PCR is the most reliable method for quantitation of HIV DNA in clinical samples. Co-amplification of competitor provides an internal control for amplification efficiency. However, the available competitor DNA is currently designed to be used in single-round PCR, which needs subsequent hybridization to obtain sufficient sensitivity. We describe here a competitive nested PCR assay for quantitation of HIV-1 gag-region. We chose the primer pairs SK380-SK390 and SK38-SK39 in our competitive nested PCR because they amplify a very conserved region and have been used routinely for quanlitative detection of HIV-1 DNA in our laboratory. The new competitor was

constructed and optimized for competitive nested PCR with high sensitivity and did not need hybridization. Our PCR system could detect at least 3 copies of HIV-1 DNA.

HIV-1 proviral DNA copy level in unsorted CD4+ T cells had a broad range from 85 to 6,734 copies/ 10^5 CD4+ T cells with a median of 389 copies/ 10^5 CD4+ T cells. This result was in agreement with previous report (108), which showed HIV-1 proviral DNA ranged between 10^3 to 10^5 copies per 10^6 CD4+ T cells. Patients with CD4 count less than 200 cell/mm^3 had about 8-fold more proviral DNA than those patients did did with CD4 count more than 200 cell/mm^3. Previous studies demonstrated that increase in viral load correlate with disease progression (99,100). Our data is consistent with previous studies, there was a significant correlation between increasing proviral DNA and a decreasing CD4 count.

In this study, we also measured the amount of HIV-1 proviral DNA in CCR5+CD4+ and CCR5-CD4+ T cell subsets. The amount of HIV-1 proviral DNA in CCR5+CD4+ and CCR5-CD4+ T cells had a broad range from 201 to 3,921 copies/ 10^5 CD4+ T cells and 24 to 5,157 copies/ 10^5 CD4+ T cells with a median of 851 and 296 copies/ 10^5 CD4+ T cells, respectively. The HIV-1 proviral DNA in CCR5-CD4+ T cells is inversely correlated with CD4 count, whereas no correlation is found between proviral DNA in CCR5+CD4+ T cells and their CD4 count. These results suggested that viruses that infect CCR5-CD4+ T cells correlated with depletion of CD4+ T cells, as defined by the CD4 count. In addition, previous data indicated that HIV-1 could enter naïve CD4+ T cells in vivo and initiate reverse transcription but are unable to integrate into the genome as efficiently as in memory CD4+ T cells (43). Recent *in vitro* studies have also demonstrated that CD45RA+CD4+ T cells can be infected with HIV-1 but are less efficient in replicating virus upon physiologic

stimulation (109,45). In our study, the HIV-1 proviral DNA was found in CCR5-CD4+ T cells from patients with different stages of disease suggested that HIV-1 could enter these cells and reverse transcribed efficiently *in vivo*.

The HIV-1 proviral DNA loads in CCR5+CD4+ and CCR5-CD4+ T cell subsets were compared within individual patients. Within a given patients there are a median of twofold higher HIV-1 proviral DNA load in CCR5+CD4+ T cells than in CCR5-CD4+ T cells. Our result similar to previous data showing that the memory CD4+ T cells contained more proviral DNA than the naïve CD4+ T cells (42,43,110).

We analyzed the ratio of HIV-1 proviral load within CCR5+CD4+ and CCR5-CD4+ T cell subsets. Higher ratio was found in patients with CD4 count more than 200 cell/mm^3, and the ratio decreased and reversed in patients with CD4 count less than 200 cell/mm^3. This ratio of HIV-1 proviral load in CCR5+CD4+ and CCR5-CD4+ T cell subsets is similar to previous studies (111). The reversed ratio suggested that in early stage of disease, as defined by the high number of CD4 count, the virus preferential infection of CCR5+CD4+ T cells and expand to infect CCR5-CD4+ T cells when disease progression. The correlation between ratio of HIV-DNA in CCR5+CD4+ and CCR5-CD4+ T cells and CD4 count might be useful marker of disease progression. Previous studies have suggested that, in early stage of infection most viruses can use CCR5, where as viruses in late stage of disease expand to use CXCR4 (10,11). In this study, most of CCR5 negative T cells expressed CXCR4. Thus, increasing proviral DNA in CCR5-CD4+ T cells in patients with low CD4 count suggest that the viruses used CXCR4 in addition to CCR5 in late stage of disease.

To predict HIV-1 phenotype, V1V2 and V3 regions were determined by PCR-direct sequencing and the viral phenotype were predicted from the deduced amino acid

sequences. In this study, we found 10 predicted SI and 18 predicted NSI viruses based on V3 sequence and all of them were grouped as subtype E. There was no correlation between V1 or V2 sequences and prediction of viral phenotype by V3 sequence and the HIV-DNA ratio, including to length, a number of potential N-link glycosylation sites, and number of positively charged residues. This result suggested that V2, V2 sequences did not effect the viral phenotype which is consistent with previous report (75).

NSI and SI viruses use different receptors for entry of target cells, the NSI viruses use CCR5, while SI viruses use both CCR5 and CXCR4. We studied the correlation between predicted viral phenotype and the distribution of HIV-1 proviral DNA load in CCR5+CD4+ and CCR5-CD4+ T cell subsets. The result showed that the ratio of CCR5+CD4+ and CCR5-CD4+ load in predicted SI individuals was lower than that ratio in predicted NSI individuals. Recent data demonstrated that CCR5 is expressed mainly on CD45RO+CD45RA- memory and activated cells where as CXCR4 is expressed mainly on CD45RO-CD45RA+ naïve cells (12,15). Thus, within the CD4+ T lymphocyte compartment, CD45RO+CD45RA- T cells express NSI coreceptor and CD45RO-CD45RA+ T cells express SI coreceptor. By this concept our result is consistent with previous data which showed that CD45RA+ load/CD45RO+ load ratio in individuals with both NSI and SI variants was higher than the ratio in individuals with only NSI variants (111). Our result suggest that the NSI or CCR5 using viruses preferential infection of CCR5+CD4+ T cells, while SI or CXCR4 using viruses preferential infection of CCR5-CD4+ T cells. Recent studies showed that the activated CXCR4+CD4+ T cells were increased in HIV-1 infected individuals (15,16).

The availability of these target cells for SI or CXCR4 using viruses may evolve the viruses from NSI/CCR5 using viruses to SI/CXCR4 using viruses.

In this study, we found some patients who were infected by predicted NSI virus had low level of proviral DNA load ratio and low CD4 count. This finding suggested that, the disease may progress even when the viruses remain to be NSI. This result is consistent with recent report (112), which showed that the majority (89%) of HIV-1 isolates in T lymphocyte from patients at all stages of infection were NSI and M tropic viruses. Moreover, the majority (87%) of all isolates, including those from patients with advanced disease, uses CCR5 for entry. These results suggest that a switch in phenotype or coreceptor usage are not essential for the enhanced replication or disease progression. Why the HIV-DNA load in CCR5 negative cells increased in some sample with predicted NSI viruses is not clear. It might indicate that the current phenotypic prediction is not accurate. However, these viral phenotype should be confirmed by co-culture with the MT-2 T cell line. Alternatively, the infection of CCR5 negative cells by R5 viruses might be due to the ability of these viruses to use CCR5 at subdetectable concentration. Pervious data showed that, a small subset of primary HIV-1 R5 strains were able to infect CD4+ T-cell lines, Molt4 and SupT1, which contained CCR5 mRNA but were negative for CCR5 by immunofluorescence staining (113). Thus the low level of proviral load ratio were found in patients with predicted NSI may describe by this concept.

CHAPTER VII

CONCLUSION

The present study can be concluded as follows.

✪ There was inversely correlation between proviral DNA in unsorted CD4+ T cells and CD4 counts with Spearman's coefficients of -0.85, $p = 0.01$.

✪ The patients with CD4 count more than 200 cells/mm^3 had a median of proviral DNA in unsorted CD4+ T cells lower than those with CD4 count lower than 200 cells/mm^3 with $p<0.01$, Mann-Whitney U test.

✪ No correlation was found between CD4 count and proviral DNA in CCR5+CD4+ T-lymphocyte ($r = -0.33$, $p = 0.072$)

✪ The patients with CD4 count more than 200 cells/mm^3 had a median of proviral DNA in CCR5+CD4+ T cells lower than those with CD4 count lower than 200 cells/mm^3 with $p=0.02$, Mann-Whitney U test.

✪ There was an inversely correlation between CD4 count and proviral DNA in CCR5-CD4+ T-lymphocyte ($r = -0.87$, $p<0.01$).

✪ The patients with CD4 count more than 200 cells/mm^3 had a median of proviral DNA in CCR5-CD4+ T cells lower than those with CD4 count lower than 200 cells/mm^3 with $p<0.01$, Mann-Whitney U test.

✪ The ratio of proviral DNA in CCR5+CD4+ and CCR5-CD4+ was correlated with CD4 count ($r = 0.76$, $p<0.01$)

✪ The ratio of proviral DNA in CCR5+CD4+ and CCR5-CD4+ T cell subset in individuals with predicted SI virus were less than in individuals with predicted NSI virus (p=0.07, Mann-Whitney U test).

✪ However, among those samples with low HIV-DNA in CCR5+CD4+/ CCR5-CD4+ ratio, about only half of them showed SI predicted phenotype (4 out of 9 samples with ratio <1 and 10 out of 20 with ratio < 5).

✪ Some patients who were infected by predicted NSI virus had low level of HIV-DNA in CCR5+CD4+/ CCR5-CD4+ ratio and low CD4 count.

REFERENCES

1. Feng Y, Broder CC, Kennedy PE, Berger EA. HIV-1 entry cofactor: funtional cDNA cloning of a seven-transmembrane, G protiencoupled receptor. Science 1996;272:872-7.

2. Alkhatib G, Combadiere C, Broder CC, Feng Y, Kennedy PE, Murphy PM, *et al.* CC CKR5: A |RANTES,MIP-1α, MIP-1β receptor as a fusion cofactor for macrophage-tropic HIV-1. Science 1996;272:1955-8.

3. Deng H, Liu R, Ellmeier W, Choe S, Unutmaz D, Burkhart M, *et al.* Indentification of a major co-receptor for primary isolates of HIV-1. Nature 1996;381:661-6.

4. Dragic T, Litwin V, Allaway GP, Martin SR, Huang Y, Nagashima KA, *et al.* HIV-1 Entry into CD4$^+$ cells is mediated by the chemokine receptor CC-CKR-5. Nature 1996;381:667-73.

5. Doranz BJ, Rucker J, Yi Y, Smyth RJ, Samson M, Peiper SC, *et al.* A dual-tropic primary HIV-1 isolate that uses fusin and the β-chemokine receptors CKR-5, CKR-3, and CKR-2b as fusion cofactors. Cell 1996;85:1149-58.

6. Choe H, Farzan M, Sun Y, Sullivan N, Rollins B, Ponath PD, *et al.* The β-chemokine receptors CCR3 and CCR5 facilitate infection by primary HIV-1 isolates. Cell 1996;85:1135-48.

7. Bleul CC, Farzan M, Choe H,Parolin C, Clark-Lewis I,Sodroski J, Springer TA. The lymphocyte chemoattractant SDF-1 is a ligand for LESTR/fusin and blocks HIV-1 entry. Nature 1996;382:829-33.

8. Oberlin E, Amara A, Bacheleric F, Bessia C, Virelizier JL, Arenzana-Seisdedos F, *et al*. The CXC chemokine SDF-1 is the ligan for LESTR/fusin and prevents infection by T-cell line adapted HIV-1.

9. Berger EA, Doms RW, Fenyo EM, Korber BTM, Litman DR, Moore JP, *et al*. A new classification for HIV-1. Nature 1998;391:240.

10. Broder CC, and Collman RG. Chemokine receptor and HIV. J Leukocyte Biol 1997;62:20-9.

11. Connor RI, Sheridan KE, Ceradini D, Choe S, and Landau NR. Change in coreceptor use correlates with disease progressiion in HIV-1 infected individuals. J Exp Med 1997;185:621-8.

12. Bleul CC, Wu L, Hoxie JA, Springer TA, Mackay CR. The HIV coreceptors CXCR4 and CCR5 are differentially expressed and reguleted on human T lymphocytes. Proc Natl Acad Sci USA 1997;94:1925-30.

13. Lee B, Shabron M, Montaner LJ, Weissman D, Doms RW. Quantification of CD4, CCR5, and CXCR4 levels on lymphocyte subsets, dendritic cells, and differentially conditioned monocyte-derived macrophages. Proc Natl Acad Sci USA 1999;96:5215-20.

14. Mo H, Monard S, Pollack H, Ip J, Rochford G, Wu L, *et al*. Expression patterns of HIV type 1 coreceptors CCR5 and CXCR4 on CD4+ T cells and monocytes from cord and adult blood. AIDS Res Hum Retroviruses 1998;14:607-17.

15. Ostrowski MA, JustementSJ, CatanzaroA, Hallahan CA, Ehler LA, Mizell SB, *et al*. Expression of chemokine receptors CXCR4 and CCR5 in HIV-1 infected and uninfected individuals. J immunol 1998;161:3195-201.

16. Auewarakul P, Sangsiriwut K, Pattanapanyasat K, Suwanagool S, and Wasi C.

Increase in Activated CD4+ Lymphocytes with CCR5 and CXCR4 in HIV

Type 1-Infected Persons. AIDS Res Hum Retroviruses 1999;15(15):1403-4.

17. Barre-Sinoussi F, Chermann JC, Rey F, Nugeyre MT, Chamaret S, Gruest J, *et al.*

Isolation of a T-lymphotropic retrovirus from a patient at risk for acquired

immune deficiency syndrome (AIDS). Science 1983;220(4599):868-71.

18. Wain-Hobson S, Sonigo P, Danos O, Cole S, Alizon M. nucleotide sequence of the

AIDS virus, LAV. Cell 1985;40(1):9-17.

19. Gallo RC, Salahuddin SZ, Popovic M, Shearer GM, Kaplan M, Haynes BF, *et al.*

Frequent detection and isolation of cytoplathic retroviruses (HTLV-III) from

patients with AIDS and at risk for AIDS. Acience 1984;224(4648):500-3.

20. Levy JA, Hoffman AD, Kramer SM, Landis JA, Shimabukuro JM, Oshiro LS.

Isolation of lymphocytopathic retroviruses from San Francisco patients with

AIDS. Science 1984;225(4664):173-7.

21. Gonda MA, Wong-Staal F, Gallo RC, Clements JE, Narayan O, Gilden RV.

Sequence homology and morphologic similarity of HTLV-III and visna virus,

a pathogenic lentivirus. Science 1985;227(4683):173-7.

22. Coffin J, Hasse A, Levy JA, Montagnier L, Oroszlan S, Teich N, *et al.* Human

immunodeficiency viruses [letter]. Science 1986;232(4751):697.

23. Louwagie J, McCutchan FE, Peeters M, Brennan TP, Sanders-Buell E, Eddy GA,

et al. Phylogenetic analysis of *gag* genes from 70 international HIV-1 isolates

provides evidence for multiple genotypes. AIDS 1993;7(6):769-80.

24. Louwagie J, Janssens W, Mascola J, Heyndrickx L, Hegerich P, van der Groen G,

et al. Genetic diversity of the envelope glycoprotein from human immunodeficiency virus type 1 isolates of African origin. J Virol 1995;69 (1):263-71.

25. Janssens W, Heyndrickx L, Fransen K, Motte J, Peeters M, Nkengasong JN, *et al.* Genetic and phylogenetic analysis of *env* subtypes G and H in central Africa. AIDS Res Hum Retroviruses 1994;10(7):877-9.

26. Kostrikis LG, Bagdades E, Cao Y, Zhang L, Dimitriou D, Ho DD. Genetic analysis of human immunodeficiency virus type 1 strains from patients in Cyprus: identification of a new subtype designated subtype I. J virol 1995;69 (10):6122-30.

27. Charneau P, Borman AM, Quillent C, Guetard D, Chamaret S, Cohen J, *et al.* Isolation and envelope sequence of a highly divergent HIV-1 isolate; definition of a new HIV-1 group. Virology 1994;205(1):247-53.

28. Simon F, Mauclere P, Roques P, Loussert-Ajaka I, Muller-Trutwin MC, Saragosti S, *et al.* Identification of a new human immunodeficiency virus type 1 distinct from group M and group O. Nat Med 1998;4(9):1032-7.

29. Unchsak K, Thanprasertsuk S, Sriparpundh S, Pinichpongse S and Kunasol P. Trends of HIV spreading in Thailand detected by National Sentinel Serosurveillance. In:Seventh International Conference on AIDS; 1991; Abs.M.C.3246.

30. Siraprapasiri T, Thanprasertsuk S, Rodklay A, Srivanichakorn S, Sawanpanyalert P, Temtanarak J. Risk factors for HIV among prostitutes in Chiangmai. Thailand. AIDS 1991;5:579-82.

31. Yu X, Yuan X, Matsuda Z, Lee TH, Essex M. The matrix protein of human

immunodeficiency virus type 1 is required for incorporation of viral envelope protein into mature virion. J Virol 1992;66(8):4966-71.

32. Coffin JM. HIV population dynamics in vivo: implications for genetic variation, pathogenesis and therapy. Science 1995;267:483-9.

33. Chan DC, Fass D, Berger JM, and Kim PS. Core structure of gp41 from the HIV envelope glycoprotein. Cell 1997;89:263-73.

34. Turner BG, Summers MF. Structural biology of HIV. J Mol Biol 1999;285(1):1-32.

35. Kwong PD, Wyatt R, Robinson J, Sweet RW, Sodroski J, and Hendrickson WA. Structure of an HIV gp 120 envelope glycoprotein in complex with the CD4 receptor and a neutralizing human antibody. NATURE 1998;393:648-59.

36. Fouchier RA, Groenink M, Kootstra NA, Tersmette M, Huisman HG, Miedema F, Schuitemaker H. Phenotype-associated sequence variation in the third variable domain of the human immunodeficiency virus type 1 gp120 molecule. J Virol 1992 ;66(5):3183-7.

37. Hwang SR, Boyle TJ, Lyerly K, and Cullen BR. Identification of the envelope V3 loop as the primary determinant of cell tropism in HIV-1. Science 1992;253:71-4.

38. De Jong JJ, De-Ronde A, Keulen W, Tersmette M, and Goudsmit J. Minimal requirement for the human immunodeficiency virus type 1 V3 domain to support the syncytium-inducing phenotype: analysis by single amino acid substitution. J Virol 1992;66:6777-80.

39. Bhattacharyya D, Brooks BR, and Callahan L. Positioning of positively charged residues in the V3 loop correlates with HIV type 1 syncytium- inducing phenotype. AIDS Res Hum Retroviruses 1996;12:83-90.

40. Speck RF, Wehrly K, Platt EJ, Atchison RE, Charo IF, Kabat D, *et al*. Selective employment of chemokine receptors as human immunodeficiency virus type 1 coreceptor determined by individual amino acid with in the envelope V3 loop. J Virol 1997;71:7136-9.

41. Rizzuto CD, Wyatt R, Hernandez RN, Sun Y, Kwong PD, and Hendrickson WA. A conserved HIV gp120 glycoprotein structure involved in chemokine receptor binding. Science 1998;280:1949-53.

42. Cayota A, Vuiller F, Scott-Algara D, and Dighiera G. Preferential replication of HIV-1 in memory CD4+ subpopulation. Lancet 1990;336:941-2.

43. Helbert MR, Walter J, L' Age J, Beverley PC. HIV infection of CD45RA+ and CD45RO+D4+ T cells. Clin Exp Immunol 1997: 107(2) 300-5.

44. Schnittman SM, Lane HC, Greenhouse J, Justement JS, Baseler M, and Fauci AS. Preferential infection of CD4+ memory T cells by human immunodeficiency virus type 1: evidence for a role in the selective T-cell functional defects observed in infected individual. Proc Natl Acad Sci USA 1990;87:6058-62.

45. Spina CA, Prince HE, and Richman DD. Preferential replication of HIV-1 in the CD45 RO memory cell subset of primary CD4 lymphocytes in vitro. J Clin Investig 1997;99:1774-85.

46. Perelson AS, Neumann AU, Markowitz M, Leonard JM, and Ho DD. HIV-1 Dynamic in Vivo: Virion Clearance Rate, Infected Cell Life-Span, and Viral Generation Time. Science 1996;271:1582-6.

47. Ho DD. Dynamics of HIV-1 Replication In Vivo. J Clin Invest 1997;99(11):2565-7.

48. Chun TW, Carruth L, Finzi D, Shen X, DiGiusppe JA, Taylor H, *et al*.

Quantification of latent tissue reservoirs and total body viral load in HIV-1 infection. Nature 1997;387:183-8.

49. Pierson T, McArthur J, and Siliciano RF. RESERVOIRS FOR HIV-1: Mechanisms for Viral Persistence in the Presence of Antiviral Immune Responses and Antiretroviral Therapy. Annu Rev Immunol 2000;18:665-708.

50. Valentin A., Albert J, Fredriksson R, Fenyo EM, and B. Sjo BA. Dual tropism for lymphocytes and mononuclear phagocytes is a common feature of primary HIV-isolates. J Virol 1994;68: 6684-9.

51. Moore JP, and Ho DD. HIV-1 neutralization: the consequences of viral adaptation to growth on transformed T cells. AIDS 1995; 9(suppl A):S117-S36.

52. Tersmette M, De Goede REY, Al BJ, Winkel I, Gruters B, Cuypers HT, *et al*. Differential syncytium-inducing capacity of human immunodeficiency virus isolates: frequent detection of syncytium-inducing isolates in patients with acquired immunodeficiency syndrome (AIDS) and AIDS-related complex. J Virol 1988;62: 2026-32.

53. Fenyo EM, Morfeldt-Manson L, Chiodi F, Lind A, von Gegerfelt A, Albert J, *et al*. Distinct replicative and cytopathic characteristics of human immunodeficiency virus isolates. J Virol 1988;62: 4414-9.

54. Koot M, Vos AHV, Keet RPM, de Goede REY, Dercksen W, Terpstra FG, *et al*. HIV-1 biological phenotype in long-term infected individuals evaluated with an MT-2 cocultivation assay. AIDS 1992;6: 49-54.

55. Asjo B, Morfeldt-Manson L, Albert J, Biberfeld G, Karlsson A, Lidman K, *et al*. Replicative capacity of human immunodeficiency virus from patients with varying severity of HIV infection. Lancet 1986; 660-2.

56. Collman R, Balliet JW, Gregory SA, Friedman H, Kolson DL, Nathanson N, *et al.* An infectious molecular clone of anunusual macrophage-tropic and highly cytopathic strain of human immunodeficiency virus type 1. J Virol 1992;66:7517-21.

57. Tersmette M, De Goede RE, Al BJ, Winkel IN, Gruters RA, Cuypers HT, *et al.* Differential syncytium-inducing capacity of human immunodeficiency virus isolates: frequent detection of syncytium-inducing isolates in patients with acquired immunodeficiency virus variants and risk for AIDS and AIDS-related complex. J Virol 1998;62:2026-32.

58. Van't Wout AB, Blaak H, Ran LJ, Brouwer M, Kuiken C, and Schuitemaker H. Evolution of syncytium-inducing and non- syncytium-inducing biological virus clones in relation to replication kinetics during the course of human immunodeficiency virus type 1-infection. J Virol 1998;72:5099-107.

59. Zhang L, Huang Y, He T, Cao Y, and Ho DD. HIV-1 subtype and second receptor use. Nature 1996;383:768.

60. Bjorndal A, Deng H, Jansson M, Fiore JR, Colognesi C, Karlsson A, *et al.* Co-receptor usage of primary human immunodeficiency virus type 1 isolates varies according to biological phenotype. J Virol 1997;71: 7478-87.

61. Simmons G, Wilkinson D, Reeves JD, Dittmar MT, Beddows S, Weber J, *et al.* Primary, syncytium-inducing human immunodeficiency virus type 1 isolates are dual-tropic and most can use either Lestr or CCR5 as co-receptors for virus entry. J Virol 1996;70: 8355-60.

62. Bjorndal A, Deng H, Jansson M, Fiore JR, Colognesi C, and Karlsson A.

Coreceptor Usage of Primary Human Immunodeficiency Virus Type 1 Isolate Varies According to Biological Phenotype. J Virol 1997;71:7478-87.

63. Willey RL, Theodore TS, and Martin MA. Amino acid substitutions in the human immunodeficiency virus type 1 gp 120 V3 loop that change viral tropism also alter physical and functional properties of the virion envelope. J Virol 1994;68 (7):4409-19.

64. Verrier F, Borman AM, Brand D, and Girard M. Role of the HIV type 1 glycoprotein 120 V3 loop in determining coreceptor usage. AIDS Res Hum Retroviruses 1999;15(8):731-43.

65. Kato K, Sato H, and Takebe Y. Role of naturally occurring basic amino acid substitutions in the human immunodeficiency virus type 1 subtype E envelope V3 on viral coreceptor usage and cell tropism. J Virol 1999;73(7):5520-6.

66. Speck RF, Wehrly K, Platt EJ, Atchison RE, Charo IF, and Kabay D. Selective Employment of Chemokine Receptors as Human Immunodeficiency Virus Type 1 Coreceptor Determined by Individual Amino Acid within the Envelope V3 Loop. J Virol 1997;71:7136-9.

67. Yu XF, Wang Z, Beyrer C, Celentano DD, Khamboonruang C, and Allen E. Phenotypic and genotypic characteristic of human immunodeficiency virus type 1 from patients with AIDS in northen Thailand. J Virol 1995;69:4649-55.

68. Wang Z, Lyles CM, Beyrer C, Celentano DD, Vlahor D, and Natpratan C. Diversification of subtype E human immunodeficiency virus type 1 *env* in heterosexual seroconverters from northen Thailand. J Infect Dis 1998; 178:1507-11.

69. Auwanit W, I.N. Ayuthaya P, Duangchanda S, Mukai T, Kurata T, and Ikuta K.

Highly Variable Sequences in the *env* V3 Region of HIV Type 1 Distributing among Thai Carriers from 1995 to 1997. AIDS Res Hum Retroviruses 2000;16 (3):283-9.

70. Groenink M, Fouchier RAM, Broersen S, Baker CH, Koot M, and van't Wout AB. Relation of Phenotype Evilution of HIV-1 to Envelope V2 Configulation. Scienc 1993;260:1513-6.

71. Koito A Harrowe G, Levy JA, and Cheng-Mayer C. Small amino acid sequence changes within the V2 domain can effect the function of a T-cell line tropic human immunodeficiency virus type 1 envelope gp120. Virology 1995; 206:878-84.

72. Palmer C, Balfe P, Fox D, May JC, Frederiksson R, and Fenyo EM. Functional Characterization of the V1V2 Region of Human Immunodeficiency Virus Type 1. Virology 1996;220:436-49.

73. Carrillo A, and Ratner L. Cooperative effects of Human Immunodeficiency Virus Type 1 Envelope Variable Loops V1 and V3 in Mediating Infectivity for T Cells. J Virol 1996;70:1310-6.

74. Andeweg AC, Leeflang P, Osterhaus AD,and Bosch ML. Both the V2 and V3 regions of the human immunodeficiency virus type 1 surface glycoprotein functionally interact with other envelope regions in syncytium formation. J Virol 1993;67:3232-9.

75. Wang N, Zhu T, and Ho DD. Sequence Diversity of V1 and V2 Domains of gp120 from Human Immunodeficiency Virus Type 1: Lack of Correlation with Viral Phenotype. J Virol 1995;69:2708-15.

76. Shioda T, Oka S, Xin X, Liu H, Harukuni R, and Kurotani A. In vivo sequence

variability of human immunodeficiency virus type 1 envelope gp120: association of V2 extension with slow disease pogression. J Virol 1997;71 (7):4871-81.

77. Maddon PJ, Dalgleish AG, Mc Dougal JS, Clapham PR, Weiss RA, and Axel R. The T4 gene encodes the AIDS virus receptor and is expressed in the immune system and the brain. Cell 1986;47:333-48.

78. Clapham PR, Blanc D, and Weiss RA. Specific cell surface requirements for the infection of CD4-positive cell by human immunodeficiency virus types 1 and 2 and by simian immunodeficiency virus. Virology 1991;181:703-15.

79. Ashorn PA, Berger EA, and Moee B. Human immunodeficiency virus envelope glycoprotein/CD4-mediated fusion of nonprimate cells with human cells. J Virol 1990;64:2149-56.

80. Choe H, Farzan M, Sun Y, Sullivan N, Rollins B, Ponath PD, et al. The beta-chemokine receptors CCR3 and CCR5 facilitate infection by primary HIV-1 isolates. Cell 1996;85:1135-48.

81. Deng HK, Unutmaz D, KewalRamani VN , and Littman DR. Expression cloning of new receptors used by simian and human immunodeficiency viruses (see comments). Nature 1997;388:296-300.

82. Doranz BJ, Rucker J, Yi Y, Smyth RJ, Samson M, Peiper SC, et al. A dual-tropic primary HIV-1 isolate that uses fusin and the beta- chemokine receptors CKR-5, CKR-3, and CKR-2b: as fusion cofactors. Cell 1996;85:1149-58.

83. Farzan M, Choe H, Martin K, Marcon L, Hofmann W, Karlsson G, et al. Two

orphan seven-transmembrane segment receptors which are expressed in : CD4-positive: cells support simian immunodeficiency virus infection. J Exp Med 1997; 186:405-11.

84. Liao F, Alkhatib G, Peden KW, Sharma G, Berger AE, Farber JM *et al.* STRL33, A novel chemokine receptor-like protein, functions as a fusion cofactor for both macrophage-tropic and T cell line-tropic HIV-1. J Exp Med 1997;185:2015-23.

85. Reeves JD, McKnight A , Potempa S, Simmons G, Gray PW, Power CA, *et al.* CD4-independent infection by : HIV-2:(ROD/B) use of the 7-transmembrane receptors CXCR-4, CCR-3, and V28 for entry. Virology 1997;231:130-4.

86. Rucker J, Edinger AL, Sharron M, Samson M, Lee B, Berson JF, *et al.* Utilization of chemokine receptors, orphan receptors, and herpesvirus encoded receptors by diverse human and simian immunodeficiency viruses. J Virol 1997;71:8999-9007.

87. Samson M, Edinger A, Rucker J, Verhasselt V, Sharron M, Govaerts C, *et al.* ChemR23: a putative chemoattractant receptor, is expressed in dendritic cells and is a coreceptor for SIV and some primary HIV-1 strains. Submitted: 1997.

88. Liu R, Paxton WA, Choe S, Ceradini D, martin Sr, Horuk R, *et al.* Homozygous defect in HIV-1 coreceptor accounts for resistance of some multiple-exposed individuals to HIV-1 infection. Cell 1996;86:367-77.

89. Samson M, Libert F, Doranz BJ, Rucker J, Liesnard C, Farber Cm, *et al.* Resistance to HIV-1 infection in caucasian individuals bearing mutant alleles of the CCR-5 chemokine receptor gene. Nature 1996;382:722-5.

90. Dean M, Carrington M, Winkler C, Huttley GA, Smith MW, Allikmets R, *et al*. Genetic resistance of HIV-1 infaction and progression to AIDS by a deletion allele of the CKR5 structural gene. Science 1996;273:1856-62.

91. Michael NL, Chang G, Louie LG, Mascola JR, Dondero D, Birx DL, *et al*. The pole of viral phenotype and CCR-5 gene defects in HIV-1 transmission and disease progression. Nat Med 1997;3:338-40.

92. Kostrikis LG, Huang Y, Moore JP, Wolinsky SM, Zhang L,Guo Y, *et al*. A chemokine receptor CCR2 allele delays HIV-1 disease progression and is associated with a CCR5 promoter mutation. Nat Med 1998;4:350-3.

93. Winkler C, Modi W Smith MW, *et al*. Genetic restiction of AIDS pathogenesis by an SDF-1 chemokine variant. Science 1998;279:389-93.

94. Wu L, Paxton WA, Kassam N, Ruffing N, Rottman JB, Sullivan N, *et al*. CCR5 levels and expression pattern correlate with infectability by Macrophage-tropic HIV-1, in vitro. J Exp Med 1997;185:1681-91.

95. Tuttle DL, Harrison JK, Anders C, Sleasman JW, Goodenow MM. Expression of CCR5 increases during monocyte differentiation and directly mediated macrophage susceptibility to infection by human immunodificiency virus type1. J Virol 1998;72:4962-9.

96. Kozak SL, Platt EJ, Madani N, Jr FEF, Peden K, and Kabat D. CD4, CXCR-4, and CCR-5 dependencies for infection by primary patient and laboratory-adapted isolates of human immunodeficiency virus type 1. J Virol 1997;71:873-82.

97. Cohen J. Searching for markers on the AIDS trail. Science 1992;258:388-390.

98. Fahey JL, Taylor JMG, Detels R, *et al*. The prognostic value of cellular and

serologic markers in infected with human immunodeficiency virus type 1 RNA. J Infect Dis 1994;170:553-62.

99. Ho DD, Moudgil T, Alam M. Quantitation of human immunodeficiency virus type 1 in the blood of infeted persons. N Engl J Med 1989;321:1621-5.

100. Ferre F, Moss RB, Daigle A, Richieri SP, Jensen F, and Carlo DJ. Viral load in Peripheral Blood Mononuclear Cells as Surrogate for Clinical Progression. J Acquir Immune Defic Syndr 1995;10:S51-6.

101. Piatak M, Jr, Saag MS, Yang LC, Clark SI, Kappes JC, Luk KC, et al. High levels of HIV-1 in plasma during all stages of infection determined by competitive PCR [See comments]. Science 1993;259(5102):1749-54.

102. Saag MS. Use of Virologic Markers in Clinical Practice. J Acquir Immune Defic Syndr 1997;16:S3-13.

103. Michael NL, Vahey M, Burke DS, and Redfield RR. Viral DNA and m RNA expression correlate with the stage of human immunodeficiency virus (HIV) type 1 infection in humans: evidence for viral replication in all stages of HIV disease. J Virol 1992;66:310-6.

104. Stieger M, Demolliere C, Ahlborn-Laake J, and Mous J. Competitive polymerase chain reaction assay for quantitation of HIV-1 DNA and RNA. J Virol Methods 1991;34:149-60.

105. Menzo S, Bagnarelli P, Giacca M, Manzin A, Varaldo PE, and Clementi M. Quantitation of viremia in Human Immunodeficiency Virus Infection by Competitive Reverse Transcription and Polymerase Chain Reaction. J Clin Micro 1992;30:1752-7.

106. Lefebvre B, Formstecher P, and Lefebvre P. Improvement of the Gene Splicing

Overlap (SOE) Method. BioTechniques 1995;2:186-8.

107. Sambrook J, Fritsch EF, and Maniatis T. Commonly Used Techniques in

Molecular Cloning. In Nolan C, editor. Molecular Cloning A

LABORATORY MANUAL. Second edition. USA: Cold Spring Harbor

Laboratory Press;

989:E5-E7.

108. Montaya JG, Wood R, Katzenstein D, Holodny M, and Merigan TC. Peripheral

Blod Mononuclear Cell Human Immunodeficiency Virus Type 1 Proviral

DNA Quantification by Polymerase Chain Reaction: Relationship to

Immunodeficiency and Drug Effect. J Clin Micro 1993;31:2692-6.

109. Roederer M, Raju PA, Dipendra KM, and Herzenberg LA. HIV does not replicate

in naïve CD4 T cells stimulated with CD3/CD28. J Clin Investig

1997;99:1555-64.

110. Ostrowski MA, Chun TW, Justement SJ, Motola I, Spinelli MA, Adelsberger J *et*

al. Both Memory and CD45RA+/CD62L+ Naïve CD4+ T Cells Are Infected

in Human Immunodeficiency Virus Type 1-Infected Individuals. J virol

1999;73(8):6430-5.

111. Blaak H, van't Wout AB, Brouwer M, Hooibrink B, Hovenkamp E, and

Schuitemaker H. *In vivo* HIV-1 infection of CD45RA+CD4+ T cells is

established primarily by syncytium-inducing variants and correlates with the

rate of CD4+ T cell decline. Proc Natl Acad Sci USA 2000;97:1269-74.

112. Li S, Juarez J, Alali M, Dwyer D, Collman R,Cunningham A, *et al*. Persistent

CCR5 Utilization and Enhanced Macrophage Tropism by Primary Blood

Human Immunodeficiency Virus Type 1 Isolates from Advanced Stages of

Disease and Comparison to Tissue-Derived Isolates. J Virol 1999;73 (12):9741-55.

113. Dejucq N, Simmons G, and Clapham PR. Expanded Tropism of Primary Human Immunodeficiency Virus Type 1 R5 Strains to CD4+ T-Cell Lines Determined by the Capacity To Exploit Low Concentrations of CCR5. J Virol 1999;73(9):7842-7.
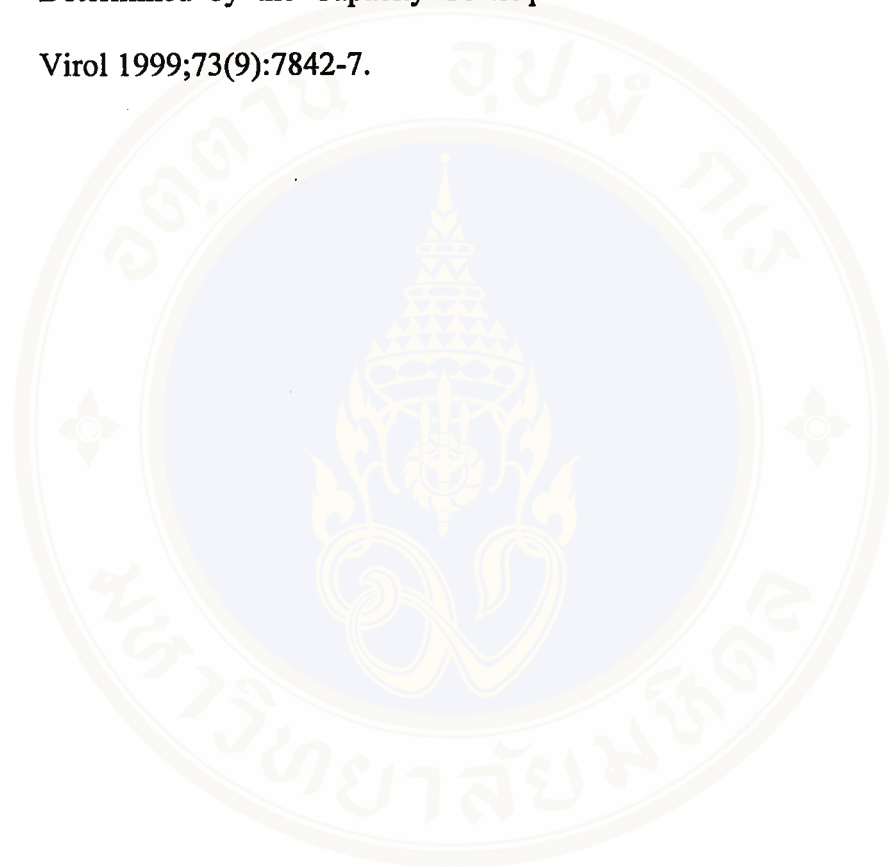
APPENDIX

Stock solution

1. 1X lysis solution

FACS® lysing solution	10 ml
Distilled water	90 ml

2. 10% paraformaldehyde

Paraformaldehyde	10 g

1X PBS to 100 ml

filttered through Whatman filter paper No.1

3. 30.8% acrylamide stock

Acrylamide	30 g
Bis-acrylamide	0.8 g
Distilled water	100 ml

filttered through Whatman filter paper No.1

4. 10% ammonium persulfate

ammonium persulfate	0.1 g
Distilled water	1 ml

Fresh preparation

Reagent for PCR Technique

1. Deoxynucleotide triphosphate (dNTPs) mixture

   Each dATP, dGTP, dCTP, and dTTP is supplied in a vial of concentration

100 mM

dATP	25 μl
dGTP	25 μl
dCTP	25 μl
dTTP	25 μl
Distilled water	900 μl

2. Loading dye (6X)

Bromphenol blue	100 μl
Sucrose	20 g
0.5X TBE buffer	50 ml

3. Ethidium bromide solution (10 mg/ml)

Ethidium bromide	1 g
Distilled water	100 ml

   Store in the dark at room temperature

4. 0.5X TBE buffer

TBE powder	8.5 g
Distilled water	1000 ml

5. 1% agarose gel

Agarose gel	0.3 g
0.5X TBE buffer	30 ml

6. 10% acrylamide gel

30.8% acrylamide stock	3.33	ml
5X TBE	3	ml
Distilled water	3.61	ml
10% ammonium persulfate	50	µl
TEMED	5	µl
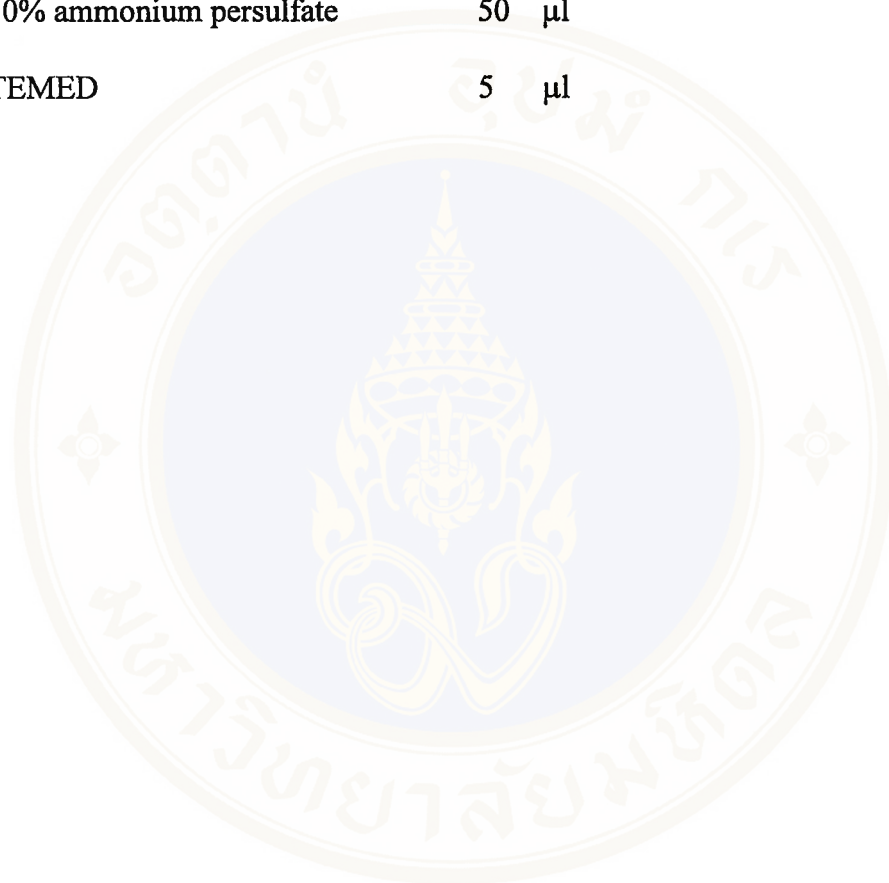
BIOGRAPHY

NAME	Miss Kantima Sangsiriwut
DATE OF BIRHT	11 July 1972
PLACE OF BIRHT	Nakornpathom, Thailand
INSTITUE ATTENDED	Mahidol University, 1991-1994:
	Bachelor of Science (Medical Technology)
	Mahidol University, 1997-2000:
	Master of Science (Microbiology)
RESEARCH GRANT	The Fogarty International Center AIDS International Training and Research Program (AITRP)
	กองทุนพัฒนาศิริราช
POSITION & OFFICE	1994 - Present,
	Infectious Disease Laboratory,
	Department of Preventive Medicine,
	Faculty of Medicine Siriraj Hospital,
	Mahidol University